

Modeling Options for Transfer Structures to Assess the Behavior of Mix Use Building Structures in High Seismic Zone

By

**Iqbal Ahmad
(MCE153016)**

**MASTER OF SCIENCE IN CIVIL ENGINEERING
(With Specialization in Structures)**



JANUARY 2017

**DEPARTMENT OF CIVIL ENGINEERING
CAPITAL UNIVERSITY OF SCIENCE & TECHNOLOGY
ISLAMABAD, PAKISTAN**

Modeling Options for Transfer Structures to Assess the Behavior of Mix Use Building Structures in High Seismic Zone

By

Iqbal Ahmad
(MCE153016)

A research thesis submitted to the Department of Civil Engineering,
Capital University of Science & Technology, Islamabad, Pakistan
in partial fulfillment of the requirements for the degree of

MASTER OF SCIENCE IN CIVIL ENGINEERING
(With Specialization in Structures)



JANUARY 2017

DEPARTMENT OF CIVIL ENGINEERING
CAPITAL UNIVERSITY OF SCIENCE & TECHNOLOGY
ISLAMABAD, PAKISTAN



C.U.S.T.

**CAPITAL UNIVERSITY OF SCIENCE & TECHNOLOGY
ISLAMABAD**

CERTIFICATE OF APPROVAL

MODELING OPTIONS FOR TRANSFER STRUCTURES TO ASSESS THE BEHAVIOR OF
MIX USE BUILDING STRUCTURES IN HIGH SEISMIC ZONE

By

Iqbal Ahmad
(MCE153016)

THESIS EXAMINING COMMITTEE

S No	Examiner	Name	Organization
(a)	External Examiner	Engr. Dr. Irshad Qureshi	UET, Taxila, Pakistan
(b)	Internal Examiner	Engr. Dr. Majid Ali	CUST, Islamabad, Pakistan
(c)	Supervisor	Engr. Dr. Munir Ahmed	CUST, Islamabad, Pakistan

Engr. Dr. Munir Ahmed

Thesis Supervisor

January, 2017

Engr. Dr. Muhammad Atiq-Ur-Rehman Tariq
Head
Department of Civil Engineering
CUST, Islamabad, Pakistan
Dated : January, 2017

Engr. Prof. Dr. Imtiaz Ahmad Taj
Dean
Faculty of Engineering
CUST, Islamabad, Pakistan
Dated : January, 2017

Certificate

This is to certify that Mr. Iqbal Ahmad (Reg # MCE153016) has incorporated all observations, suggestions and comments made by the external as well as the internal examiners and thesis supervisor. The title of his thesis is: “Modeling Options for Transfer Structures to Assess the Behavior of Mix Use Building Structures in High Seismic Zone”.

All the comments of internal and external examiner are incorporated and attached as **Annexure-A**.

Forwarded for necessary action please.

Engr. Dr. Munir Ahmed
(Thesis Supervisor)

DEDICATION

In the service of my motherland

ACKNOWLEDGMENT

1. First and foremost, I would like to pay my deepest gratitude to my supervisor, Engr. Dr. Munir Ahmed whose support, guidance and advice helped me complete this work. My experience of working with him has been an interesting and rewarding one.
2. I acknowledge from the core of my heart all those who helped me directly or indirectly in my master studies.
3. I gratefully acknowledge the financial support for my master's studies by the Capital University of Science and Technology, Islamabad.
4. Last but not the least; I extend my thanks from the core of my heart to all my family members, especially my parents, for their prayers, advice and encouragement throughout my career.

TABLE OF CONTENTS

DEDICATION	I
ACKNOWLEDGMENT.....	II
TABLE OF CONTENTS.....	III
LIST OF TABLES	V
LIST OF FIGURES	VI
LIST OF ABBREVIATIONS.....	VIII
ABSTRACT.....	IX
LIST OF INTENDED PUBLICATION	X
Chapter 1 Introduction	1
1.1 Background	1
1.2 Problem Statement	2
1.3 Objectives.....	3
1.4 Limitations of the Study.....	3
1.5 Methodology	4
1.6 Organization of Thesis	4
Chapter 2 Literature Review.....	6
2.1 Introduction	6
2.2 Euler-Bernoulli Beam Theory.....	8
2.3 Timoshenko Beam Theory	9
2.4 Codal Requirements for Design of Deep Beams	10
2.5 Behavior of Deep Beam (Shear and Flexural)	11
2.6 Finite Element Modeling (FEM) of Deep Beam.....	19
2.7 Summary of Literature Review and Research Gap.....	22
Chapter 3 Prototype Beam	24
3.1 Introduction	24
3.2 Beam Description.....	24
3.3 Different Modeling Techniques	27
3.3.1 Frame/Line Element.....	27
3.3.2 Shell/Area Element	28
3.3.3 Solid/3D Element.....	28

3.3.4	Strut and Tie Element	29
3.4	Design of Deep Beam by STM	29
3.4.1	Struts	30
3.4.2	Nodal Zones	31
3.4.3	Ties.....	32
3.5	Results and Discussion.....	33
3.6	Summary of Prototype Beam	41
Chapter 4	Case Study.....	43
4.1	Introduction	43
4.2	Description of Case Study Structure	43
4.3	Equivalent Static Analysis (ESA)	51
4.4	Response Spectrum Analysis (RSA).....	52
4.5	Results and Discussion.....	53
4.5.1	Behavior of the TG using non-linear shell layered model based on ESA	53
4.5.2	Comparison of non-linear shell layered model with other models	55
4.6	Summary of Case Study.....	65
Chapter 5	Summary, Conclusion And Recommendations	67
5.1	Summary	67
5.2	Conclusion.....	68
5.3	Limitations of the Study.....	69
5.4	Recommendations for Future Work.....	70
REFERENCES	71

LIST OF TABLES

Table 3.1. Qualitatively comparison of strain distribution diagram of non-linear shell layered element with experimental diagram in literature	35
Table 3.2. Qualitatively comparison of stress distribution diagram of non-linear shell layered element with experimental diagrams in literature.....	36
Table 3.3. Suitable modification factors	37
Table 3.4. Strain distribution diagrams for different modeling techniques	38
Table 3.5. Stress distribution diagrams for different modeling techniques	39
Table 4.1. Strain distribution diagrams at Mid-Span of different modeling techniques under gravity loading	60
Table 4.2. Strain distribution diagrams at Mid-Span of different modeling techniques under gravity plus seismic loading.....	61
Table 4.3. Stress distribution diagrams at mid-span of different modeling techniques under gravity loading	62
Table 4.4. Stress distribution diagrams at support of different modeling techniques under gravity loading.....	63
Table 4.5. Stress distribution diagrams at mid-span of different modeling techniques under gravity plus seismic loading.....	64
Table 4.6. Stress distribution diagrams at support of different modeling techniques under gravity plus seismic loading.....	65

LIST OF FIGURES

Figure 2.1. A residential building in Hong Kong having transfer structure at 1st floor level. (<i>Su, R. K. L., & Cheng, M. H. (2009)</i>).....	6
Figure 2.2. Deep beam (transfer girder), Brunswick Building, Chicago (picture courtesy of columbia.edu).....	7
Figure 2.3. Single Span Deep Beam (<i>MacGregor & Wight, 2005</i>).....	8
Figure 2.4. Infinitely long beam under end bending moments.	9
Figure 2.5. Deformation component of a Timoshenko beam element.	10
Figure 2.6. Developments of cracks in deep concrete specimen (<i>David et al., 2008</i>).....	13
Figure 2.7. Non-linear stress distribution (a) <i>Aftab (1965)</i> and (b) <i>Holmes (1972)</i>	14
Figure 2.8. Non-linear distribution (a) strains and (b) stress (<i>Niranjan and Patel, 2012</i>).....	14
Figure 2.9. Cracking along Tensile Reinforcement for Thin Beam	15
Figure 2.10. Cracking causing crushing of compression area for a deep beam <i>MacGregor & Wight (2005)</i>	15
Figure 2.11. Deep Beam Distances.....	16
Figure 2.12. Forces in vertical reinforcement increase with angle.....	17
Figure 2.13. Section of a Deep Beam Showing the Horizontal Reinforcement Resisting Cracking	17
Figure 2.14. Non-Linear Stress Distribution <i>Hassoun and Al-Manaseer (2008)</i>	18
Figure 3.1. Detail of small prototype beam	25
Figure 3.2. Different modeling techniques for prototype beam; (a) frame/line element, (b) shell/area element, (c) solid/3D element, and (d) STM.....	26
Figure 3.3. Non-linear <i>Park steel and Mander et al.'s concrete model</i>	27
Figure 3.5. Behavior of reinforcement of prototype beam at a load of 94 kips; (a) bottom reinforcement, (b) top reinforcement and (c) transverse reinforcement.....	34
Figure 3.6. Behavior of reinforcement of prototype beam at a load of 109 kips; (a) bottom reinforcement, (b) top reinforcement and (c) transverse reinforcement.....	35
Figure 3.7. Deflection of small prototype beam before and after the alignment of other models compared to that of non-linear shell layered model.....	37
Figure 4.1. (a) XZ-Elevation and (b) 3D view of the case study building	44
Figure 4.3. Architectural plans: (a) Typ. basement plan, (b) TGs layout (c) Typ. ground floor plan and (d) Typical apartments plan.....	49

Figure 4.4. Different modeling techniques of TG of case study structure (a) frame/line element, (b) thick shell/area element and non-linear shell layered element, (c) solid/3D element and (d) STM	50
Figure 4.5. Behavior of TG from non-linear shell layered element; (a) crack pattern under factored gravity loading, (b) crack pattern under gravity plus seismic loading, (c) bottom reinforcement under gravity loading, (d) bottom reinforcement under gravity plus seismic loading, (e) top reinforcement under gravity loading, (f) top reinforcement under gravity plus seismic loading, (g) shear reinforcement under gravity loading, (h) shear reinforcement under gravity plus seismic loading.....	54
Figure 4.6. Maximum deflection of TG from different modeling techniques	54
Figure 4.7. Crack pattern of; (a) thick shell element under gravity loading, (b) thick shell element under gravity plus seismic loading, (c) solid element under gravity loading and (d) solid element under gravity plus seismic loading	55
Figure 4.8. Maximum compressive stress in struts and tensile stress in ties of STM; (a) under gravity loading and (b) under gravity plus seismic loading.....	56
Figure 4.9. Storey shears of different modeling techniques for ESA	57
Figure 4.10. Storey shear of area element for RSA	57
Figure 4.11. Overturning moments of different modeling techniques for ESA	57
Figure 4.12. Overturning moments of area element for RSA.....	57
Figure 4.13. Storey drift ratios of different modeling techniques.....	58

LIST OF ABBREVIATIONS

<i>ACI</i>	American Concrete Institute
<i>FEM</i>	Finite Element Method
<i>TP</i>	Transfer Plate
<i>DBM</i>	Deep Beam Method
<i>TG</i>	Transfer Girder
<i>lc</i>	Clear span
<i>h</i>	Overall depth of the beam
<i>a/d</i>	Shear span to depth ratio
<i>UBC 97</i>	Uniform Building Code 1997
<i>STM</i>	Strut and Tie Method
<i>ESA</i>	Equivalent Static Analysis
<i>RSA</i>	Response Spectrum Analysis
<i>fc'</i>	Compressive Strength of Concrete
<i>fy</i>	Yield Strength of Steel
<i>I</i>	Moment of Inertia
<i>G</i>	Shear Modulus
<i>E</i>	Elastic Modulus
<i>h</i>	Depth of Beam
<i>b</i>	Breadth of Beam
<i>Q</i>	Shear Stress
<i>M</i>	Bending Moment
<i>ω</i>	Displacement of Mid-Surface in the Z-direction
<i>φ</i>	Angle of Rotation of the Normal to the Mid-Surface of the Beam
<i>ψ</i>	Shear Angle

ABSTRACT

In modern world due to multi-functional requirements and architectural constraints, the transfer structures in low to moderate seismic zones are being used. However, the suitable modeling options and modification factors to account the true behavior of these types of structures need to be investigated in high seismic zones. In this study, a small prototype simply supported beam having shear span to depth ratio of less than 2 has been first designed manually using strut and tie approach and then modeled using different modeling techniques such as non-linear shell layered, area element, solid element, line element and strut and tie method (STM), available in commercial software's. The cracking pattern, stress and strain distribution obtained from the different FEM modeling technique have been compared with experimental studies in the literature and on the basis of the results obtained, non-linear shell layered is selected as reference model. All other models are modified to approximately align with reference model in respect of mid span deflection. To account for the effect of cracking on stiffness, the modulus of elasticity and shear modulus of concrete is reduced by 20% in case of frame/line element. For shell/area element, moment of inertia is reduced by 35% of its gross value. For solid element, the modulus of elasticity and shear modulus of concrete is reduced by 40%. Whereas in case of STM, no stiffness modification factors are used. The findings of the small prototype are used in modeling transfer girders (TGs) in 11-storied building. The transfer girder (TG) is given at ground level and the building is founded on soil profile type-SD and located in seismic zone-04. The cracks pattern, stress and strain distribution, storey shear, overturning moments and deflections are worked out using gravity and seismic load combinations using equivalent static procedure. These parameters from each model have been compared with those obtained from the reference model in order to rank the modeling techniques. Based on this comparison, it is found that STM, thick shell, solid and line element are better modeling techniques in order of preference starting from STM. On the basis of the building performance in this study, it is confidently recommended the use of TGs in severe seismic zone-04. This research will help practicing engineers to select the best modeling technique for modeling of TG in mix use building structures.

LIST OF INTENDED PUBLICATION

Intended journal article

Ahmad, I and Ahmed, M. (2017). "Different Modeling Techniques for Transfer Structures". *Advances in Structural Engineering*. (ISI Impact Factor = 0.57), (Review in Progress)

CHAPTER 1 INTRODUCTION

1.1 Background

For modern buildings, due to multi-functional requirements and architectural constraints, the lateral force resisting systems are in common use normally consists of shear wall systems in upper floors and moment resisting frames along with basement retaining walls in lower floors. The lower floors of the buildings are normally utilized for shopping centers, get-together corridors, open spaces/platform gardens for utilitarian prerequisites, whereas the upper floors normally accommodate apartments/offices. To accommodate this arrangement, the utilization of transfer structures between the lower floors and the upper floors of a high rise building is very popular now-a-days. Transfer structure or Transfer girders (TG) which is actually a deep beam by definition, are mostly being used in mix use construction in low to moderate seismic zones. Therefore, understanding of the design processes and choosing an appropriate design process is a need for safe and economic building design. A beam which has $l_c = 4h$ (where l_c = clear span and h = overall depth of the beam) or having shear span to depth ratio less than or equal to 2, is a deep beam as per ACI-318. The ratio of clear span to overall depth of TG (also referred as Transfer structures in this study) is in general less than 4; therefore, they fall under the definition of deep beams given by ACI-318-11.

To design a deep beam, Requirements of the Building Code for Structural Concrete of American Concrete Institute (ACI 318-11) provides two methods. These methods include Strut and Tie Method (STM) and/or Deep Beam Method (DBM). The DBM method consists of an appropriate and rational way to design the cracked reinforced concrete beam based on various testing data by many researchers. The STM is a modified version of the truss analogy which includes the concrete contribution through the concept of equivalent stirrup reinforcement. The truss analogy was first introduced by Schlaich et al., 1987. Once the concrete exceeds its tensile strength, cracks will appear and all the stresses will transfer to the vertical and horizontal reinforcement across the cracks. The Pre-stressed Concrete Institute (PCI) Journal published a four part article named “Towards a Consistent Design of Structural Concrete” on the truss analogy. This generalizes the truss analogy by proposing an analysis method in the form of STMs which are

valid in all regions of the structure (Schlaich et al., 1987). The STM is included in the ACI code, ACI 318-11, in its Appendix A.

Actual stresses of a deep beam are non-linear, therefore more widely used design approach for deep beams is through a nonlinear distribution of the strain by DBM and is covered in ACI-318, Sections 10.2.2, 10.2.6, 10.7 and 11.7. Typically, a reinforced concrete beam is analyzed by a linear-elastic method and designed for the redistributed stresses after cracking. Analysis of deep beams by linear elastic method revealed that the stresses determined were less than the actual stresses near the center of the span (ACI Task Committee 426, 1973).

For the analysis of deep beams, various analytical tools are available. Among all these available analytical tools, finite element analysis (FEA) presents a better and convenient option. The FEM is a numerical procedure for the analysis of structures and continua. The classical analytical methods cannot be used for the satisfactory solution as the problem addressed is too complicated normally. The problem may be required to perform many analysis e.g. stress analysis, heat conduction, or many other areas. Digital computers are used to generate and solve many simultaneous algebraic equations which are produced by finite element procedure. Results are not too much accurate. However, the approximately exact solution may be obtained by processing these equations. Results are accurate enough for engineering purposes and obtainable at reasonable cost. To fully understand the behavior of RC deep beams, FEM is a powerful and general analytical tool (Sciarmmarella, 1963; Singh, et. al. 2008 and Tan, et. al.2003). For linear and non-linear behavior of deep beam structural elements, finite element method can provide realistic and satisfactory solutions (Quanfeny and Hoogenboom, 2004, Samir and Chris, 2005).

1.2 Problem Statement

For the prediction of deep beam behavior, either elastic theory or semi empirical equation is commonly used now-a-days. As these theories are based on linear analysis, thus they may not be acceptable (Yoo, et. al. 2007, Kong and Chemrouk, 2002). Typically, a reinforced concrete beam is analyzed and designed by linear-elastic method. A stiffness modification factor is sometimes used for the consideration of cracking effect. However, the actual stresses distribution of a deep beam is non-linear (Hassoun and Al-Manaseer, 2008). The stiffness modification factor of 0.35 given in ACI code may not be correct for deep beams. Therefore, suitable modeling

techniques, for transfer girders to assess the gravity and seismic behavior and suitable stiffness modification factors to account for the cracking effects, need to be investigated.

Currently, ACI-318 does not provide equations for the design of non-linear stress distribution. The present research program analyzes the behavior of transfer girders using different modeling techniques i.e. frame/line element, thick shell/area element, solid/3D element and STM. A small prototype deep beam (see chapter-03) has been manually designed using STM and then modeled using the above mentioned modeling techniques. The numerical modeling has been compared to other provisions/experimental studies and a reference model has been selected. All other modeling techniques have been approximately aligned to that of reference model in respect of maximum deflection. The conclusions drawn from this small prototype deep beam are extended to 11-storeid case study structure (see Chapter 04). Different parameters e.g. from case study structure for each modeling technique has been compared and best modeling technique compatible with failure mechanism and deflection of deep beam is recommended.

1.3 Objectives

The main objectives of the research program are to;

- Encourage the use of transfer structures (i.e TG) in mix use buildings in high seismic zones.
- Present suitable modeling option of transfer girders i.e. line/frame element, area/shell element, solid/3D, non-linear shell layered element and strut and tie model.
- Present suitable stiffness modification factor for the assessment of the true gravity and seismic forces in mix use building structures.
- Discuss the seismic behavior of the transfer structure.
- Recommend the best modeling technique.

1.4 Limitations of the Study

The limitations of this study are;

- Only numerical modeling, analysis and design have been done.
- Only linear equivalent static analysis (ESA) and response spectrum analysis is performed. Static pushover analysis or non-linear time history analysis is not performed.

- Different parameters are qualitatively compared with experimental work found in literature i.e. no experimental work is performed.

1.5 Methodology

To ascertain the correct modeling technique compatible with failure mechanism and deflection of deep beam and also based on time and computational effort required for the analysis, the following methodology is adopted in this study:

- A small deep beam is designed manually using STM technique. The results are then verified analytically through different modeling techniques i.e. elastic line element, shell element, solid element and non-linear shell layered element.
- Then, an 11 storied RCC structure with transfer girders at ground level, seismic zone-4 and soil profile type SD is analyzed using the above mentioned modeling techniques.
- The overall gravity and seismic behavior of the building is studied using various seismic assessment methodologies such as response spectrum analysis (RSA) and equivalent static analysis (ESA).
- Different parameters such as storey drifts, storey shears and overturning moments etc. are compared for each modeling technique.
- Total 25 numbers of simulations for small deep beam and 20 numbers of simulations are made for the case study structures.

1.6 Organization of Thesis

Chapter 2: This chapter gives a detailed review of the use of transfer structures in low to moderate seismic zones, codal requirements for the shear and flexural behavior of the deep beam and Finite Element Modeling (FEM) of deep beam.

Chapter 3: In this chapter, the small prototype beam has been discussed in detail. Different modeling techniques in commercially available software e.g. SAP2000 etc., Strut and Tie Modeling (STM) according to ACI-318 and failure mechanism of deep beam has also been discussed briefly. The cracking pattern, stress and strain distribution obtained by numerical modeling is qualitatively compared with the experimental findings available in the literature.

Chapter 4: This chapter presents a detailed discussion about the 11-storied RCC case study structure with transfer girder having a shear span to depth ratio less than 2.5 at ground level,

seismic zone-4 and soil profile type SD. The transfer girder is modeled using the mentioned modeling techniques and their effect on overall gravity and seismic behavior of the building is discussed. The response spectrum analysis (RSA) and equivalent static analysis (ESA) are also discussed. Different parameters e.g. storey drift, storey shears and overturning moments etc., are compared for modeling techniques and best modeling technique is recommended.

Chapter 5: This chapter gives the summary of the research work, conclusions drawn from the analytical work and recommendations for future studies.

CHAPTER 2 LITERATURE REVIEW

2.1 Introduction

For modern buildings, due to multi-functional requirements and architectural constraints, the basic structures are in common use which generally comprises of a system of shear wall in upper floors and moment resisting frames along with basement retaining walls in lower floors. The lower floors of the structures are generally utilized for shopping centers, get-together corridors, platform gardens/open spaces for practical necessities, whereas the upper floors generally accommodate apartments/offices. The transfer structure supports the columns and shear walls of the upper floors and redistributes their heavy loads to the supporting walls or columns below through flexural or shear action depending on the span to depth ratio of the supporting members. Many forms of transfer structures e.g. transfer plates (TP) or transfer girders (TG) may be used in high rise commercial and residential buildings. In some mega cities, which are located in the low seismicity region, for example Hong Kong, Shanghai, New York, London, Bangkok and Singapore, transfer structures are used (Su and Cheng 2009). Figure 2.1 shows a residential building in Hong Kong having transfer structure at 1st floor level.



Figure 2.1. A residential building in Hong Kong having transfer structure at 1st floor level. (Su, R. K. L., & Cheng, M. H. (2009))

Transfer girders in structures are typically deep beams. A transfer girder usually supports the loads from columns which rest above and transfers these loads to other support columns which are below the transfer girders. A common location for a transfer girder is entrances for parking garages or other unique structures where large loads are applied to a structure with an opening at a column location (see Figures 2.2 and 2.3). “In general, deep beams are regarded as members loaded on their extreme fibers in compressions. Examples of this type of member are pile caps and transfer girders. Members loaded through the floor slabs or diaphragms are closer to the conditions that are idealized for shear walls” (ACI Task Committee 426, 1973).



Figure 2.2. Deep beam (transfer girder), Brunswick Building, Chicago (picture courtesy of columbia.edu)



Figure 2.3. Single Span Deep Beam (MacGregor & Wight, 2005)

The span to depth ratio of Transfer structures i.e. TG is normally less than 4; thus, they fall under the definition of deep beams given by ACI-318-11.

ACI-318-11 provides two methods for the design of deep beams which include Strut-and-Tie Method (STM) or Deep Beam Method (DBM), in Appendix A and Sections 10 and 11, respectively. Typically, a reinforced concrete beam is designed by a linear-elastic method. The stresses determined by linear-elastic method are less than that of actual stresses for deep beam, particularly near the center of the span (ACI Task Committee 426, 1973). Currently, ACI-318 does not have equations for the design of non-linear stress distribution.

2.2 Euler-Bernoulli Beam Theory

Many theories are presented on the basis of various assumptions and prompt to various levels of exactness. One of the most useful and simplest theory, among all the available beam theories, is the one presented by Euler and Bernoulli commonly known as Euler-Bernoulli theory. The main assumption on which this theory is based is “the beam cross section is infinitely rigid in its plane and in the plane of the cross section no deformations occur”. Following are the assumptions of the Euler-Bernoulli theory in explicit form:

1. The X-section in its plane is infinitely rigid.

2. After deformation, the plane cross-section of the beam remains plane.
3. The deformed axis of the beam and X-section remains normal to each other.

The idealized problem of a long beam, which has constant properties along its span and only two bending moments is applied, is shown in Figure 2.4. The magnitudes of the bending moments applied at the ends are M .

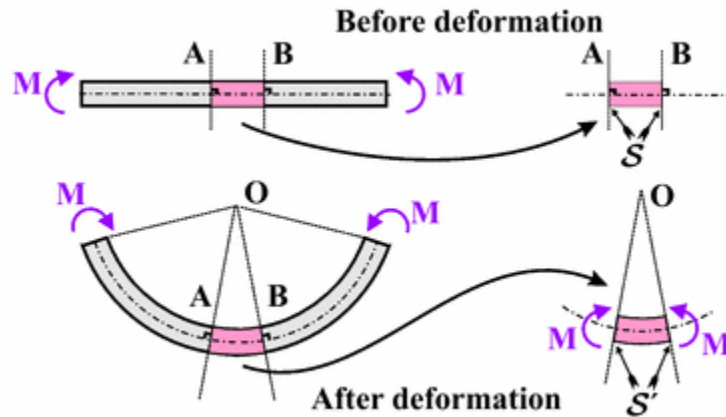


Figure 2.4. Infinitely long beam under end bending moments.

After deformation, the beam cross-sections remain normal to the deformed axis of the beam and plane, as shown above (*Bauchau and Craig, 2009*).

2.3 Timoshenko Beam Theory

The Timoshenko beam theory was developed by Stephen Timoshenko in the early twentieth century. The model considers shear deformation and rotational bending effects. It is suitable for the description of short beams behavior, sandwich composite beams, or beams where high-frequency excitation (when the wavelength approaches the thickness of the beam) is applied. The resulting output equation is of 4th order. There is also a second-order partial derivative present. The stiffness of the beam lowers by due to the added mechanism of deformation. Due to this consideration, the larger deflection (under a static load and lower predicted Eigen frequencies for a given set of boundary conditions) occurs in the output. This is more prominent for higher frequencies. The wavelength becomes shorter which ultimately results in the decrease of the distance between opposing shear forces.

Timoshenko beam theory converges towards ordinary beam theory; if (i) the shear modulus of the beam material approaches infinity and (ii) rotational inertia effects are neglected.

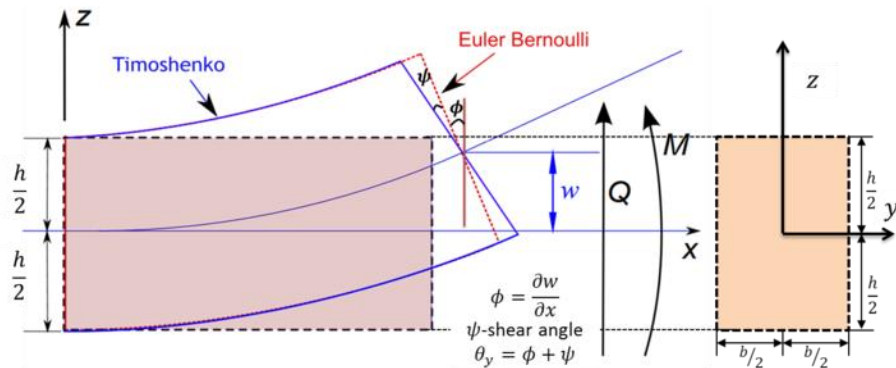


Figure 2.5. Deformation component of a Timoshenko beam element.

The design of thin beam is carried out on the basis of the Euler-Bernoulli theory (discussed above). This suggests that the rotations and axial strains of the beam are very less as compared to the depth of the beam. Due to the considerations of the effect of transverse shearing, the Timoshenko's theory is applicable for the designing of deep beam. The X-sections of the beam can be considered plane, but it is not necessary that they are normal to the axis of bending. Due to large span to depth ratio of deep beam, the strain distribution is no longer considered linear and the shear deformations become significant when compared to pure flexure (ACI Task Committee 426, 1973).

2.4 Codal Requirements for Design of Deep Beams

In the codes of practice, many modifications have been considered in the shear design of deep beams (Rao et al. 2007). For the estimation of shear strength of deep beams, ACI-318 considers the contribution of concrete, shear span to overall depth ratio, longitudinal and transverse reinforcement. British Standards (BS-8110) does not clearly give any guidelines for the design of a deep beam. However, it explicitly indicates that the design of deep beams should be supported by appropriate and valid literature. BS-8110 takes into account the effect of size in the design of shear of reinforced concrete (RC) beam. So, in order to understand the proper design approach of deep beams, serious research efforts are required. The American Concrete Institute has developed the Building Code Requirements for Structural Concrete (ACI 318) and Commentary

(ACI 318R). In code, only non-linear distribution of strain and lateral buckling is taken into account for the flexure design of deep beam. The code does contain the definition of deep beams, shear requirements which tends to govern the size (depth) of a deep beam, minimum area of flexural reinforcement, and minimum vertical and horizontal reinforcement on each face of deep beams in Sections 10.5, 10.6, 10.7, and 11.7. For the design of deep beams, these sections require the non-linear strain distribution or STM theory (ACI Committee 318, 2008).

ACI 318-11, Section 10.7.1 defines deep beams as those members which are normally loaded on one face and supports are provided on the opposite face. The mechanism is such that the compression struts can develop between the loads and the supports. ACI-318 further defines deep beams as members with one of the following to be valid:

- (a) The clear span (l_c) is equal to or less than 4 times the overall depth

$$\frac{l_n}{h} \leq 4.0$$

Where:

l_c = the clear span for distributed loads which is measured from the face of the support;

h = the overall depth of the member. *OR*

- (b) the shear span to depth ratio is less than or equal to 2.

$$\frac{a}{h} \leq 2.0$$

Where:

a = area of the beam which is loaded with the concentrated loads and measured from the face of the support.

2.5 Behavior of Deep Beam (Shear and Flexural)

High rise building structures are increasingly growing now-a-days, so introduction of deep beams in mega structures is a need to accommodate multifunctional requirements. The Euler-Bernoulli theory is not applicable to deep beams. In order to understand the structural behaviors of such beam i.e. deep beams, a lot of experimental/analytical study is available in the literature for the investigation of structural behavior and design method of the deep beam.

Many research groups have developed design method for deep beams. ACI and Euro codes, give guidance for the design of deep beams taking into account the shear behavior. The failure mode of thin beam and deep beam is flexural and shear, respectively. For deep beams, an analysis which takes into account the non-linear distribution of stresses should be used. (Park, R and Paulay, T. 1975). On the basis of strut-and tie concept, Tang and Tan (2004) offered a technique which caters the effect of transverse stresses to the load carrying capacity of concrete in the diagonal strut. Russo et al. (2005) offered an explicit expression which considers the shear strength based on strut and tie mechanism. The STM is composed of diagonal concrete strut and longitudinal reinforcement as well as vertical stirrups and horizontal shear reinforcement. Bakir et al. (2004) recommends the STM for the design of short and deep beams only. Aguilar et al. (2002) studied the behavior of RC deep beams for initial response i.e. initial flexural cracking, initial diagonal cracking, initial yield of longitudinal steel and failure. The shear strength was also predicted on the recommendations provided by ACI318-99 and compared with the provisions of ACI318-02. They concluded that both ACI318-99 and ACI318-02 are conservative, whereas the STM given in ACI318-02 is less conservative. The relationship between the applied force and the strength in the main strut and ties of deep beam was studied by Matamoros and Wong (2003). They proposed an equation which is also used for the prediction of shear strength of the deep beam. The findings of the proposed equation and the experimental results are almost equal which implies that the proposed equation is reliable. Quintero et al. (2006) performed experiments for the prediction of factors involved in concrete strut strength. The results were compared with the guidelines provided in ACI318-02 building code (Appendix-A). The Appendix-A was confirmed through the experimental finding only for normal strength concrete not for high strength concrete. The ACI318-02 gives the ultimate shear strength more than that of experimental findings (up to 10%) in high strength concrete. In addition to strut and tie mechanism, the effect of concrete softening effect caused by shear reinforcement was studied by Arabzadeh et al. (2009). Despite of the fact that the shear reinforcement influences the behavior of the deep beam, but for effective behavior of deep beam the optimized amount of shear reinforcement should be used. For the determination of the amount of shear reinforcement, the strength of concrete, span to depth ratio and main tensile reinforcement ratio may be used. For the prediction of ultimate shear strength of the deep beam, they developed a formulation. The formulation encompasses the concrete strength, arrangements & amount of shear

reinforcement and shear span to depth ratio. The shear action which consists of compression in one direction and tension in the perpendicular direction causes a disturbance in internal stresses in deep beams. This results in an abrupt failure of the beam in shear as the depth of the beam increases (Yang et al. 2003). The beams having span of 12.3ft and shear span to overall depth ratio of 1.5 tested using three-point loading. The shear failure was observed and the modes of failure were affected by the amount of shear reinforcement and depth of the beam (Rao et al. 2007). As the beam depth increases, the development of crack pattern becomes much faster which leads to abrupt failure (Bakir and Boduroglu, 2004). The shear strength reduces gradually with the increase of effective depth of beam (Iguro et al. 1984). RC deep beams failed in shear due to crushing of concrete in compression zone with restricted depth above the tip of the critical diagonal crack (Zararis, 2003). With the increase in amount of longitudinal reinforcement, significant reduction in crack width occurs (Khaldoun et al. 2004). In deep beams with a shear span to overall depth ratio of 2.5, some strength is reserved in the region of post-cracking which results in comparatively less brittle in nature (Khaldoun, 2000, Lin and Lee, 2003).

Birrcher et al. (2008) investigated the crack pattern of deep beam. The beam failure occurred due to shear failure and with the increase of the load, the diagonal cracks become wider. The same behavior is also reported by Masab et al. (2014).



Figure 2.6. Developments of cracks in deep concrete specimen (David et al., 2008)

Aftab (1965) reported the non-linear stress distribution of deep beam and the same was reported by Holmes et al. (1972), and Niranjan and Patil (2012). Niranjan and Patil (2012) also reported the non-linear strain distribution of deep beams.

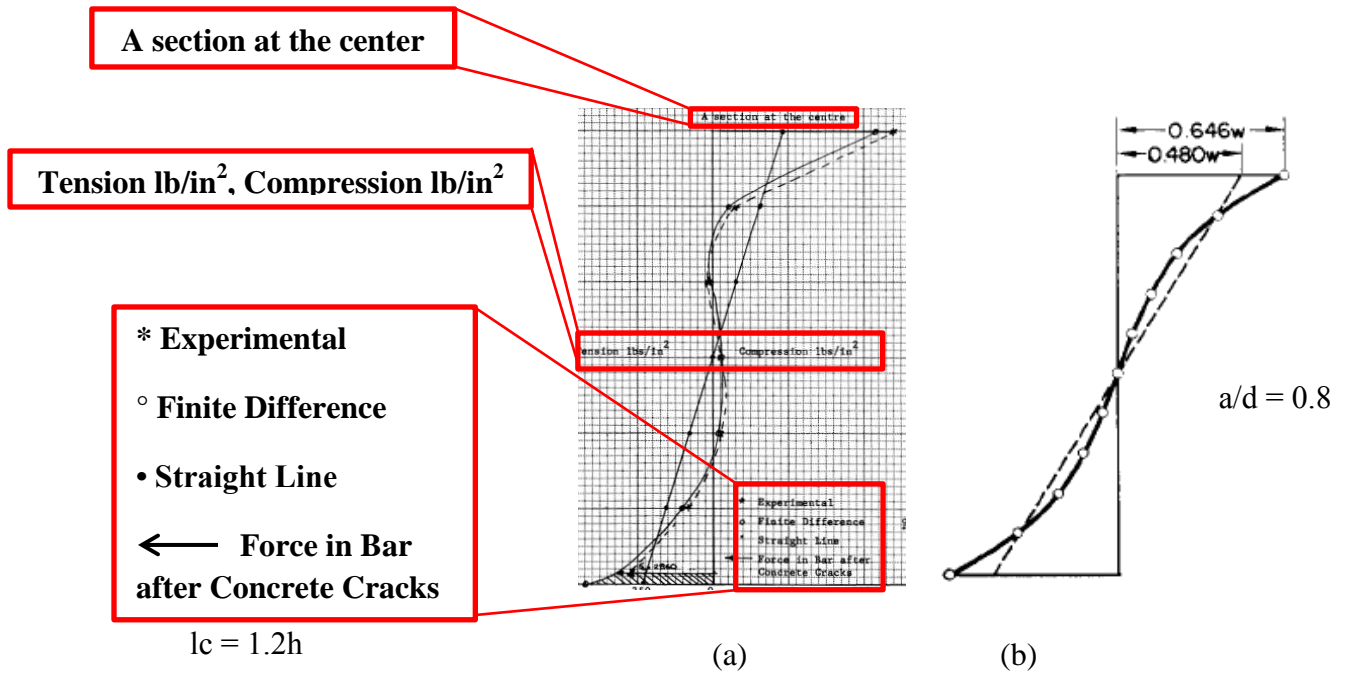


Figure 2.7. Non-linear stress distribution (a) Aftab (1965) and (b) Holmes (1972)

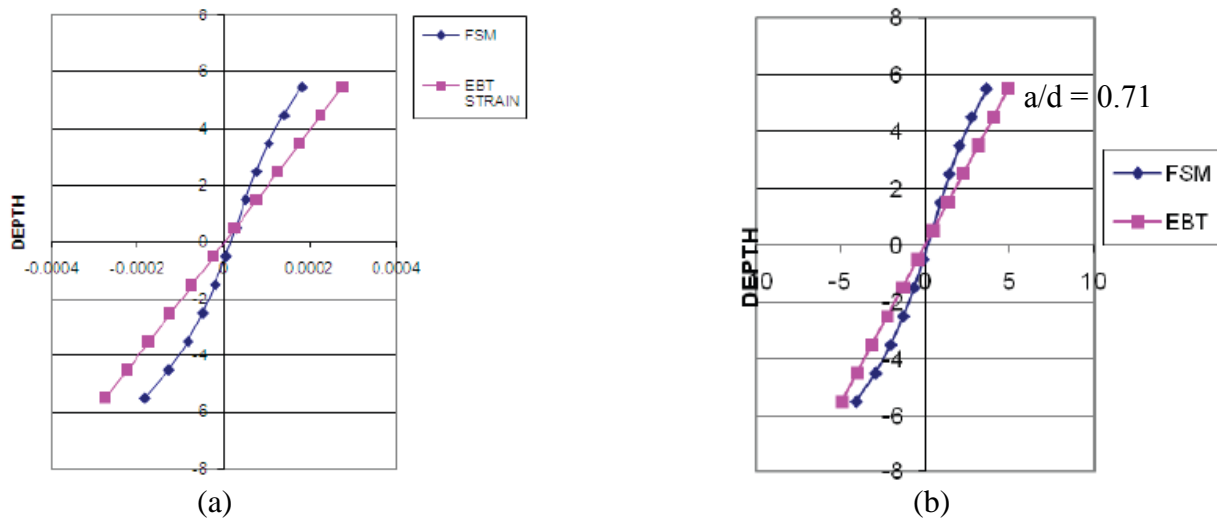


Figure 2.8. Non-linear distribution (a) strains and (b) stress (Niranjan and Patel, 2012)

In case of the application of axial loads on deep beams, there is lack of information about their behaviors. While other beams are typically governed by requirements for flexural strength, deep beams are governed by requirements for shear strength. Therefore, the first type of failure that designers should consider when designing a deep beam (to determine the depth of the beam required for shear strength) is shear failure. Shear failure occurs due to the combined shearing force and bending moment. Sometimes, occasionally, axial load, or torsion, or both can also cause the shear failure (ACI Task Committee 426, 1973). In designing a shorter member, shear typically sets the minimum depth for the beam. As the depth of a member increases, inclined cracking from shear or flexure tends to become steeper as shown in Figures 2.9 and 2.10. These steeper inclined cracks mean shear transfer mechanisms and shearing failures differ considerably from typical beams. The most common mode of shear failure is the crushing or shearing of the compression area over an inclined crack. This is typically started by cracking along the tensile reinforcement (ACI Task Committee 426, 1973). Figures 2.9 and 2.10 illustrate cracking patterns for standard beams and deep beams respectively while demonstrating the crushing shear failure that can occur in deep beams.

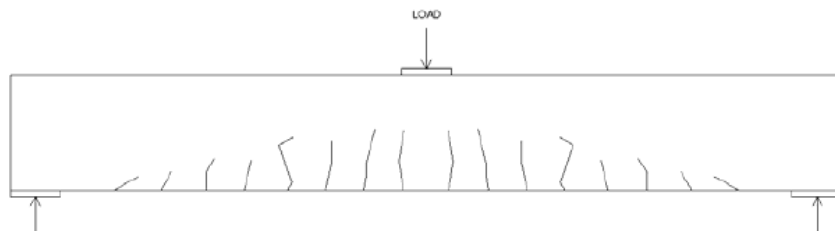


Figure 2.9. Cracking along Tensile Reinforcement for Thin Beam

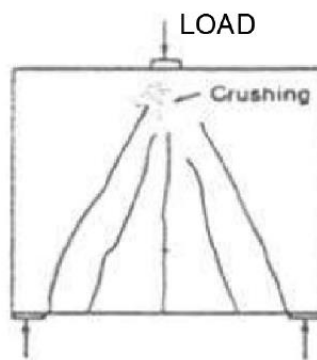


Figure 2.10. Cracking causing crushing of compression area for a deep beam MacGregor & Wight (2005)

The most important variable affecting the way a beam loaded with a concentrated load fails in shear is the ratio of a/d , the distance from the load to the edge of the support over the effective depth of the member as shown in Figure 2.11.

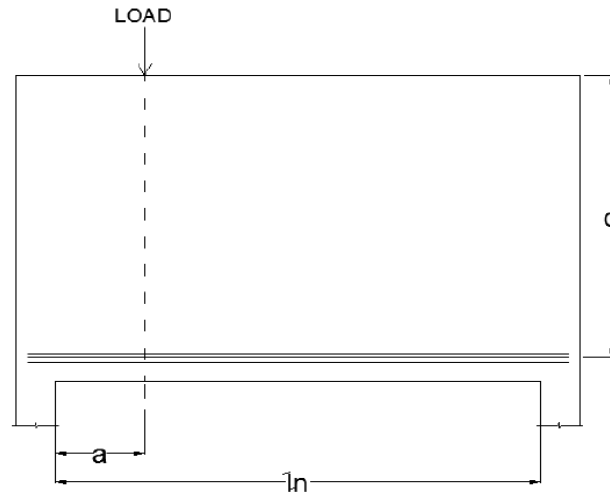
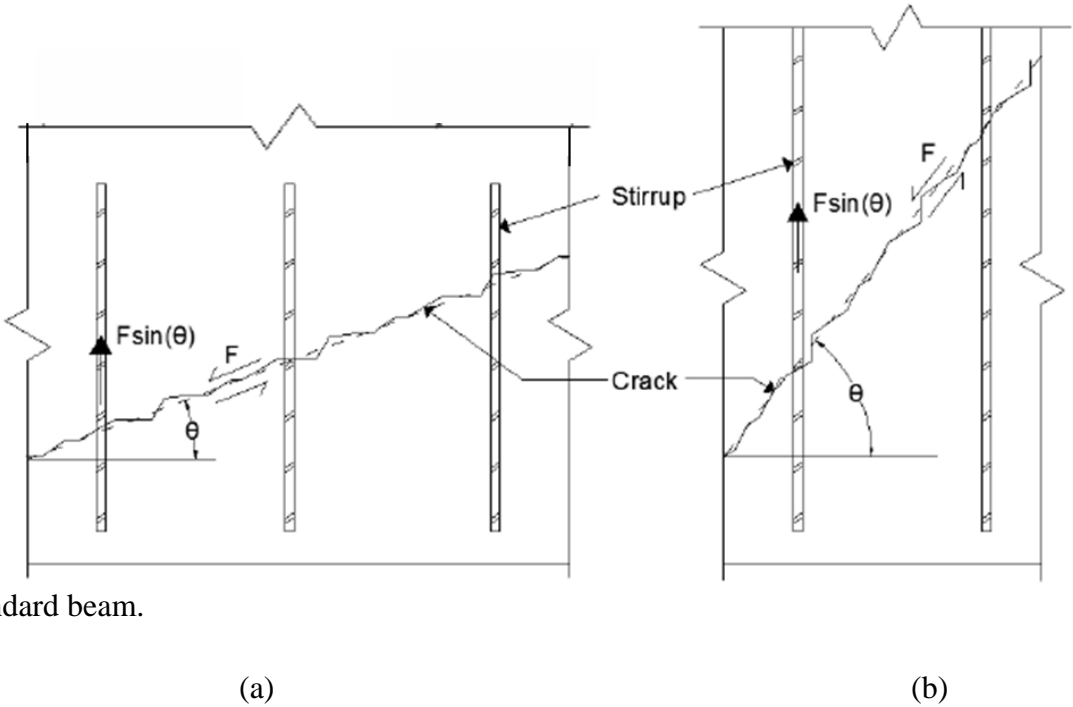


Figure 2.11. Deep Beam Distances

Furthermore, this ratio can be expressed as M/V_d , where M is the ultimate moment, and V is the ultimate shear strength at the critical section of the beam (ACI Task Committee 426, 1973). “This ratio recognizes the fact that a part of the shearing force is carried by the web reinforcement and part by the longitudinal steel. The beam is considered failed when a limit for failing stress reached in the compression zone” (Sheikh et al., 1971). A common characteristic of deep beams is a ratio of M/V_d less than 2.5 (ACI Task Committee 426, 1973). This is typically attributed to three things common to deep beams: a smaller moment, M ; a larger effective depth, d ; and a higher shear force, V .

The shear failure was observed and the modes of failure were affected by the amount of shear reinforcement and depth of the beam (Rao et al. 2007) and as the beam depth increases, the development of crack pattern becomes much faster which leads to abrupt failure (Bakir and Boduroglu, 2004). Therefore, as the ratio of a/d decreases from about 2.5 to 0, the shear reinforcement parallel to the force is less effective (ACI Task Committee 426, 1973). With the increase in depth of the member, the ratio of a/d decreases. Thus, the cracks that form become steeper with increasing depth of the beam. Due to the increase in depth the cracks become

steeper which increased the angle of the cracks. Therefore, the forces applied to the vertical shear reinforcement are increased and caused the vertical reinforcement to become less effective as shown in Figure 2.12(b). Figure 2.12(a) indicates the forces in vertical reinforcement for a



standard beam.

Figure 2.12. Forces in vertical reinforcement increase with angle

The cracks form jaggedly, leaving plenty of edges to interlock (aggregate interlock), creating a large coefficient of friction between the two edges of the crack. The horizontal reinforcement holds these cracks together or keeps them from becoming too large, thus increasing the friction between the two edges and the efficiency of the horizontal reinforcement, shown in Figure 2.13.

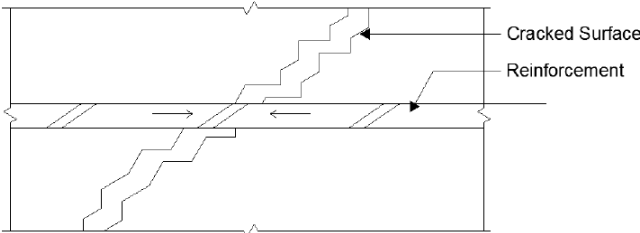


Figure 2.13. Section of a Deep Beam Showing the Horizontal Reinforcement Resisting Cracking

The flexural design of a deep beam is similar to a typical beam with a few changes to the internal moment arm and location of the tension reinforcement. The factored nominal strength, ΦM_n must be greater than the factored applied moment, M_u . The design flexural strength is calculated using the following equation:

$$\Phi M_n = \Phi A_s f_y j d$$

Where:

j = is a dimensionless ratio used to define the lever arm, jd . It varies because of varying loads;

jd = the modified internal moment arm because of non-linearity of the strain distribution, the distance between the resultant compressive force and the resultant tensile force;

$\Phi = 0.9$ for tension controlled members per ACI 318-11 Section 9.3.2.1.

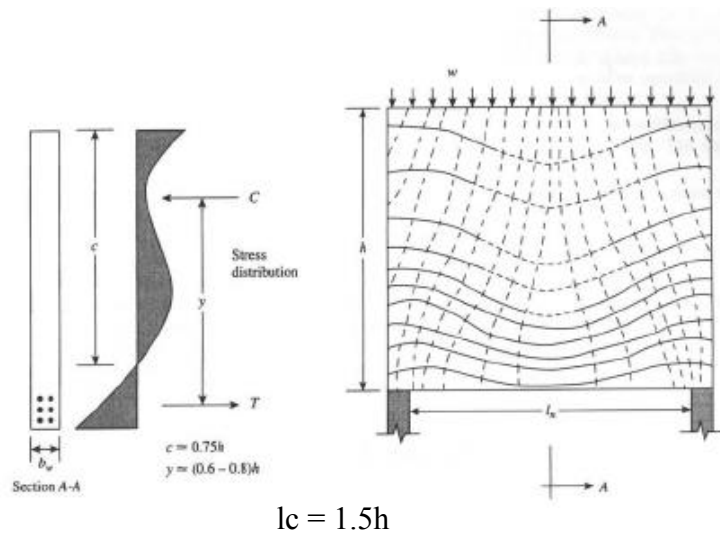


Figure 2.14. Non-Linear Stress Distribution Hassoun and Al-Manaseer (2008)

Figure 2.14 represents a deep beam and the non-linear stress distribution. C is the resultant compression force and T is the resultant tensile force. The depth of the compression block is represented by c and y represents jd which is the internal moment arm.

To determine the amount of flexural steel required, the design flexural strength is set equal to the factored moment, M_u , and solved for required area of steel, A_s ACI-318 limits the amount of

steel that can be used to ensure a ductile failure. The minimum steel requirements can be found in ACI-318 Equation 10-3, given below:

$$A_s = \frac{M_u}{\Phi f_y j d} \geq \frac{3\sqrt{f'_c} b_w d}{f_y} \geq \frac{200 b_w d}{f_y}$$

For a typical beam with a depth greater than 36 inches, skin reinforcement is required to extend to $h/2$ from the tension face to control cracking as per ACI-318-11 Section 10.6.7. The reinforcement distributed on the face helps control cracking. Without this reinforcement, the width of the cracks in the web may exceed the allowable crack widths at the flexural tension reinforcement. Before 1999, the ACI limits for crack control were based on a maximum crack width of 0.016 inch for interior exposure and 0.013 inch for exterior exposure (MacGregor & Wight, 2005). The role cracks have in corrosion of reinforcement is controversial as research has shown that they do not clearly correlate, thus, the exterior exposure requirement has been eliminated (Committee 318, 2008). ACI-318 has specified a maximum spacing of the flexure reinforcement at the face of the beam to keep cracks within the crack limits. Multiple bars of a smaller diameter are better than one bar in crack control. ACI 318-11 Equation 10-4, given below, specifies the maximum spacing in the flexural reinforcement.

$$s = 15 \left(\frac{40,000}{f_s} \right) - 2.5c_c \leq 12 \left(\frac{40,000}{f_s} \right)$$

Where:

C_c = least distance from the surface of reinforcement steel to the tension face;

f_s = permitted to be taken as $2/3f_y$ per ACI 318-11 Section 10.6.4.

2.6 Finite Element Modeling (FEM) of Deep Beam

For the basic formulation of flexural beam models, two theories are used. The Euler-Bernoulli theory, which is a classical theory, is used for thin beams. The basic assumptions of this theory are that, after loading (a) the X-sections of the beam remain plane and (b) normal to the axis of bending. The Timoshenko's theory is used for deep beams. This theory takes into account the

effect of transverse shearing deformations. According to this theory, the assumption (a) for Euler-Bernoulli theory may be valid but assumption (b) is not valid. In case of deep beams, one reason for the transferring of significant amount of load to the supports by compression strut, which joins the load and the reaction, is the large overall depth to span ratio. Due to this transfer of load, the strain distribution is no longer assumed linear. Also, as compared to pure flexural, the shear deformations are significant.

The first order linear load deflection relationship is normally used for the analysis of reinforced concrete structures or deep beams and the strains developed in the structures are assumed small. This means that the geometric non-linearity is not taken into account. So the real behavior and the computed behavior of the member differ from each other normally, which ultimately lead to approximate solutions. The exact figure for the difference in results, when geometric nonlinearity is taken into account, is not known. It is obvious that plain concrete has a little resistance to crack propagation due to low tensile strength and limited amount of ductility. In case of compression, about one-third of the ultimate strength is occupied by these micro-cracks propagation. In case of tension (approximately to one-tenth of the compressive strength) brittle failure is occurred due to these cracks.

Existing methods used for the prediction of deep beam behavior is either based on elastic theory or semi-empirical formulation, none of them is entirely satisfactory (Yoo, et. al. 2004, Kong and Chemrouk, 2002).

In recent years, various proposals have been floated for the design of reinforcement for in-plane forces based on the lower bound limit state approach where a stress field in equilibrium at the ultimate load is used in conjunction with an appropriate yield criterion. Such a stress field can be obtained by any suitable procedure such as a linear elastic finite element analysis. Reinforcement is then provided so that the combined resistance of the steel and concrete at every point is equal to or greater than the applied stress.

In theory, by satisfying equilibrium and yield exactly at every point simultaneously, the entire structure will become a mechanism at ultimate load. Practical considerations, such as reinforcement being provided as discrete bars, make it impossible to achieve this idealized

behavior. Also, the theory gives no guarantee that serviceability behavior will be satisfactory. However, if verified as an acceptable design process, the following advantages ensure:

- analysis and design becomes one continuous process which is suited to automatic computation.
- steel is used economically as the design equations are based on minimizing steel requirements, although this will be affected by the convenience of fabrication;
- excessive ductility demands are minimized by aiming for most parts of the structure to yield simultaneously at a particular ultimate load. The difference between the load at which yielding starts and the ultimate load is kept at a reasonable level which should prevent excessive cracking at working load.

Verification for practical reinforcement details can be provided by non-linear finite element modeling of the resulting designs, backed up by large experimental tests.

For the analysis of deep beams, various analytical tools are available. Among all these available analytical tools, finite element analysis (FEA) presents a better and convenient option. The FEM is a numerical procedure for the analysis of structures and continua. The classical analytical methods cannot be used for the satisfactory solution as the problem addressed is too complicated normally. The problem may be required to perform many analysis e.g. stress analysis, heat conduction, or many other areas. Digital computers are used to generate and solve many simultaneous algebraic equations which are produced by finite element procedure. Results are not too much accurate. However, the approximately exact solution may be obtained by processing these equations. Results are accurate enough for engineering purposes and obtainable at reasonable cost. The FEA usually involves the following steps;

- Division of the structure or continuum into finite elements. Mesh generation's programs, which are known as preprocessors, help the user in doing this work.
- Formulation of the properties of each element.
- Assembling of elements to obtain the FEM of the structure.
- Application of the known loads, nodal forces and/or moment in stress analysis.
- In case of stress analysis, specification of the supporting mechanism of the structure. This step involves setting many nodal displacements into known values.

- Solution of the simultaneous linear algebraic equations for the determination of nodal degree of freedom (DoF).
- In case of stress analysis, calculation of the element strains from the nodal DoF and the element displacement field interpolation, and finally calculation of stress from strains.

Many elements are used for the analysis of any continuum in case of FEM, which is a laborious and time consuming by manual calculations. The manpower and effort required to prepare the relevant and necessary data and interpret the results increase as the number of elements increases. Therefore, computer based programs help to reduce the effort and fatigue involved by analyzing a continuum by manual analysis. Some programs may be limited from the solution of a large number of finite elements to idealize the continuum. Engineers/designers are now capable to model, analyze and design innovative complex and unusual structures on the basis of the availability of advanced analysis tools using finite elements and matrix structural analysis concepts. To fully understand the behavior of RC deep beams, FEM is a powerful and general analytical tool (Sciarmmarella, 1963; Singh, et. al. 2008 and Tan, et. al.2003). For linear and non-linear behavior of deep beam structural elements, finite element method can provide realistic and satisfactory solutions (Quanfeny and Hoogenboom, 2004, Samir and Chris, 2005). Computer based programs are used to reduce the effort and fatigue involved in manual analysis. The following factors influence the effectiveness of a program: (i) the use of efficient finite elements, (ii) efficient programming methods and effective use of the available computer hardware and software, and (iii) a very important aspect is the use of appropriate numerical techniques (Klus, 1990, Enem, et al., 2012). Many modeling techniques i.e. frame/line element, area/shell element, solid/3D element, STM and non-linear shell layered element, are available in commercially available software's e.g. SAP2000, ETABS etc.

2.7 Summary of Literature Review and Research Gap

Literature review and research gap may be summarized as follows:

- The TG, which is actually a deep beam, is used in some mega cities which are located in low to moderate seismic regions. The TG is used due to multifunctional requirements or some architectural constraints. A common location for a TG is entrances for parking

garages or other unique structures where large loads are applied to a structure with an opening at a column location.

- The clear span to depth ratio of deep beam is less than or equal to 4 as per ACI-318. The clear span to depth ratio of TG is normally less than 4; therefore they fall under the definition of deep beams as per ACI-318 definition.
- ACI-318 provides DBM and STM for the design of deep beams but due to the availability of FEM package software, new design strategy needs to be adopted.
- In the codes of practice, many modifications have been made. ACI-318 considers contribution of concrete, shear span to overall depth ratio, and longitudinal and transverse reinforcement. BS-8110 provides no clear guidelines regarding deep beams.
- The failure mode is dominated by flexural failure in case of thin beams whereas by shear failure in deep beams as reported in previous studies. Thin beams are based on Euler Bernoulli's theory and deep beams are based on Timoshenko's theory. In case of Euler Bernoulli's theory the plan section is assumed to remain plane after loading and the deformed axis of the beam and X-section remains normal to each other. In case of deep beam the above said assumptions are not valid and hence Timoshenko's theory is applicable.
- FEM is a powerful and general analytical tool (Sciarmmarella, 1963; Singh, et. al. 2008 and Tan, et. al.2003). For linear and non-linear behavior of deep beam structural elements, finite element method can provide realistic and satisfactory solutions (Quanfeny and Hoogenboom, 2004, Samir and Chris, 2005). Computer based programs are used to reduce the effort and fatigue involved in manual analysis.

Many modeling techniques are available in commercially available software's, however the suitable modeling techniques compatible with the behavior of deep beams need to be investigated. In this research program, the suitable modeling technique to assess the gravity and seismic behavior of TG and suitable modification factors are recommended.

CHAPTER 3 PROTOTYPE BEAM

3.1 Introduction

The main objective of this study is to present the suitable modeling techniques and stiffness modification factor of transfer girders for the assessment of the true gravity and seismic forces in reinforced cement concrete (RCC) structures. In order to meet the objective, a small deep beam having shear span to depth ratio less than 2.5, designed manually by STM, and analyzed by different modeling techniques to ascertain the correct modeling technique compatible with failure mechanism and deflection of deep beams. The conclusions drawn from this small prototype deep beam are applied to a case study structure (see Chapter 04) and on the basis of the results found, best modeling technique is recommended for the modeling and designing of transfer girder. This chapter focuses on the description of prototype beam, different modeling techniques and comparison to experimental results.

3.2 Beam Description

A small prototype simply supported beam of 49 inches length and 18 inches depth is selected. The compressive strength of concrete (f_c') is 6,000 psi and the yield strength of steel is 60,000 psi. The reinforcement detail of small prototype beam, worked out manually for two points loading of 30 kips applied at a distance of 20 inches using strut and tie approach of ACI-318-11, is shown in Figure 3.1. The truss analogy for STM is taken from the recommendation of FU (2001) as a good modeling option. The STM as per the provisions of ACI 318-11 (see section 3.4) is used for the designing of small prototype beam. The shear force is calculated from the shear force diagram. Using the geometry and shear force of the strut and tie model of deep beam, the forces in struts and ties are calculated. The following formula is used for the calculation of area of steel in tie element:

$$F_{nt} = \phi A_{st} f_y$$

Where:

F_{nt} = Force in tie element;

A_{st} = Area of steel required in tie;

f_y = Yield strength of the steel used.

For the calculation of shear reinforcement, the following formula is used:

$$A_v = 0.0025b_wS_v$$

Where:

b_w = Effective width of the beam;

A_v = Area of rebar to be used in shear reinforcement;

S_v = Spacing of shear reinforcement.

In this case, the force calculated in tie is 30.08 kips. Using the formula for the calculation of reinforcement in tie, 2-#5 bars are selected as tension reinforcement. The 2-#4 bars are provided at the top as a minimum reinforcement.

The above formula is used for the calculation of shear reinforcement spacing and #2 bars are used at a spacing of 3.5".

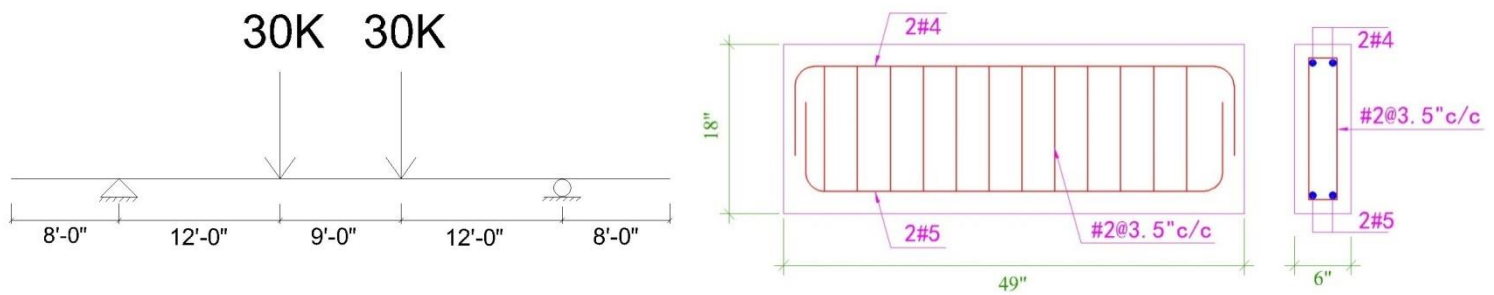


Figure 3.1. Detail of small prototype beam

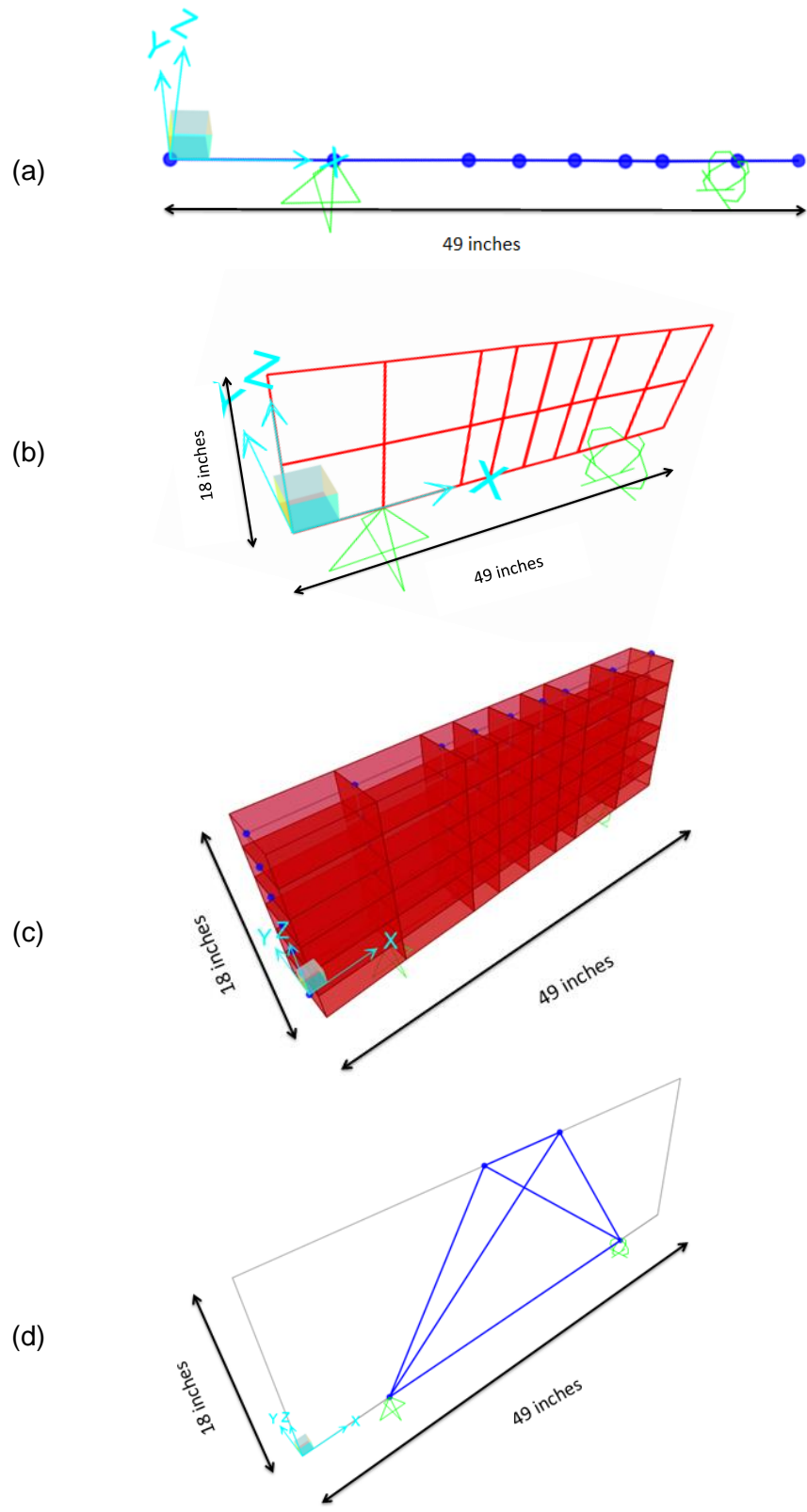


Figure 3.2. Different modeling techniques for prototype beam; (a) frame/line element, (b) shell/area element, (c) solid/3D element, and (d) STM

The moment of inertia of beam is reduced by 35% of gross moment of inertia to account for the effect of cracking as per ACI-318-11, except in non-linear shell layered model where cracking effects are automatically taken into account because of non-linear material modeling and analysis. The load is applied gradually in increments. At the start, two point loads having magnitude of 30 kips are applied at a distance of 20 inches from both edges of the beam. The load is increased arbitrarily from 30 kip to 47 kips, 78 kips, 94 kips and 109 kips finally. As the reinforcement yielded at a load of 109 kips, further loading the beam is stopped. Steel reinforcement and concrete stress-strain relationship proposed by Mander et al. (1984) are assigned to re-bars and concrete, respectively, in non-linear shell layered model to account for non-linear behavior. The stress strain relationships are shown in Figure 3.3.

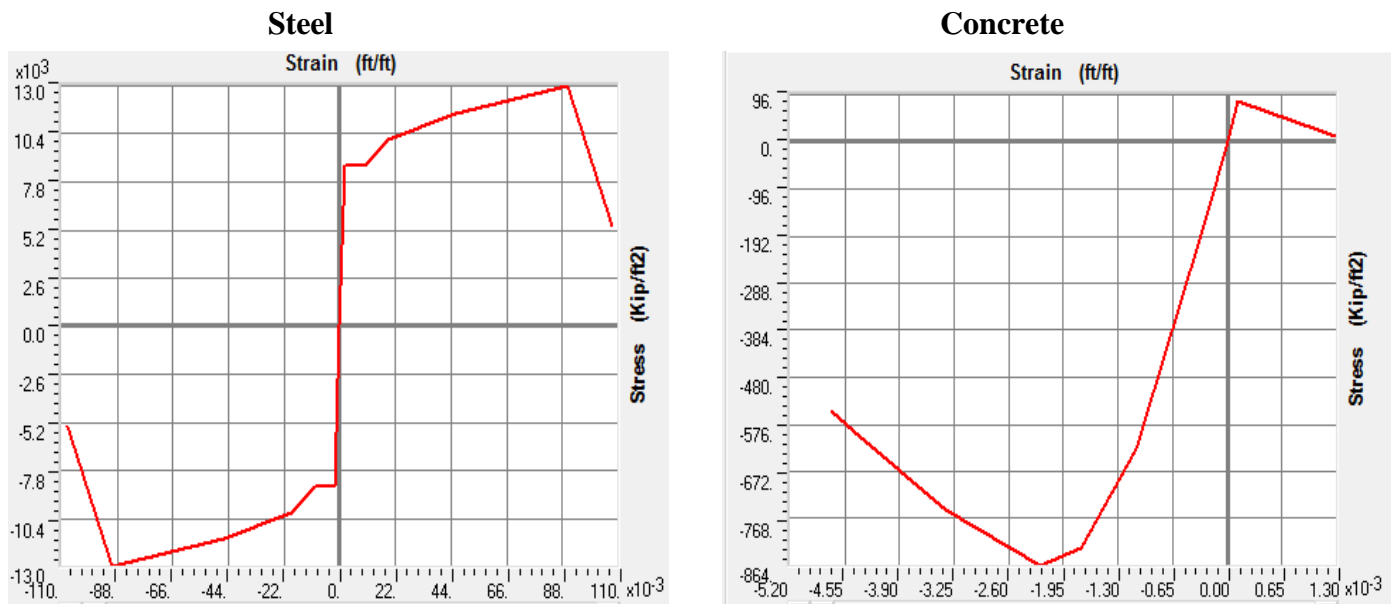


Figure 3.3. Non-linear Park steel and Mander et al.'s concrete model

3.3 Different Modeling Techniques

3.3.1 Frame/Line Element

The frame element uses a general, three-dimensional, beam-column formulation which includes the effects of biaxial bending, torsion, axial deformation, and biaxial shear deformations (Bathe and Wilson, 1976). This type of the element is designed by the ultimate strength design of ACI-

318-11 code. This method of the design is based on Euler-Bernoulli thin beam theory in which linear strain distribution is assumed (CSI analysis reference manual, 2011).

3.3.2 Shell/Area Element

3.3.2.1 Thick Shell Element

The thick shell elements have both in-plane stiffness and out-of plane stiffness. In case of non-planer element, in-plane and out-of-plane behaviors become coupled. For the modeling of each homogenous shell element in the structure, pure membrane, pure plate, or full shell behavior may be used. For non-planer element, the full shell behavior is generally recommended, unless the entire structure is planer and is adequately restrained. The material for thick shell/area element is modeled as linear and homogenous (CSI analysis reference manual, 2011).

3.3.2.2 Non-linear shell layered Element

In layered shell, material nonlinearity can be considered. To define number of layers in the thickness direction, each with an independent location, thickness, behavior, and material, the layered shell is used. A Mindlin/Reissner formulation is used for bending which always includes transverse shear deformations. Although layered shell can be controlled on a layer-by-layer basis, this usually represents full shell behavior. Actual stress-strain relationship of the materials used in different layers can be incorporated; therefore, this model may be the most suitable technique for assessing the true behavior of the deep beams as the material non-linearity and strain distribution across thickness can be incorporated using rebar and concrete layers (CSI analysis reference manual, 2011).

3.3.3 Solid/3D Element

To model the three dimensional solid structures, the solid element is used. The solid element is an eight- node element. The difference in values calculated from different elements attached to common joints are used to evaluate approximate error in the stresses. Based on this indication of the accuracy of the finite element approximation, a new and more accurate finite element mesh can be selected. The solid/3D modeling is based on Timoshenko's theory, where non-linearity of strain distribution may also be taken into account by solid element (CSI analysis reference manual, 2011).

3.3.4 Strut and Tie Element

In Strut-and-Tie method, model is idealized as a system of strut, tie and node (ACI-318-11). The strut is a compression member and made of concrete, whereas tie or stirrup is a tension member and made of steel reinforcement. The node connects the strut with ties and made of concrete. Compression struts serve as (1) the compression chord of the truss mechanism which resists moment, (2) diagonal struts which transfer shear to the supports in the STM. Diagonal struts are generally oriented parallel to the expected axis of cracking. Tensions ties include stirrups, longitudinal (tension chord) reinforcement, and any special detailed reinforcement. Nodes are the connections of the STM, i.e., the locations at which struts and ties converge. A STM developed with struts parallel to the orientation of initial cracking will behave very well. There is no single, unique STM for most design situations encountered. There are, however, some techniques and rules, which help the designer to develop an appropriate model. According to ACI-318, the minimum angle of strut is $\theta_{\min} = 25^\circ$; ($25^\circ \leq \theta$ recommended $\leq 65^\circ$). If small θ is assumed in the truss model, the compression strength of the inclined strut is decreased (FU, 2001).

3.4 Design of Deep Beam by STM

The design of an STM consists of laying out a truss that fits within the deep beam with the appropriate cover while being able to transfer the forces without failing. ACI 318-11, Appendix A, specifies some strength and geometry limitations and design equations. The internal factored forces, F_u , must be less than the design strength represented by ACI 318-11 Equation A-1, i.e.

$$\phi F_n \geq F_u$$

The first step in the design process is to determine beam dimensions. Typically, the beam width will be governed or equal to the column dimensions to which it is connected. To determine the height of the beam, the ultimate factored shear load applied on the beam must be known. The angle between the strut and the tie needs to be considered at this time as well. ACI 318-11, Section A.2.5 states that the angle, θ , between any strut and tie must not be less than 25° or greater than 65° in order to “mitigate cracking and to avoid incompatibilities” in the nodal regions due to shortening of the struts and lengthening the ties occurring in the same direction. The optimum angle to keep nodal regions and struts to a reasonable size is $40-45^\circ$. As the angle increases, the force in the strut decreases requiring less strut width; however, to increase the

angle, the beam depth must be increased. As the angle increases past 45°, increasing the angle becomes less effective because the difference in the force in the strut from angle to angle decreases in value.

Once the beam dimensions have been selected, deep beam criteria should be checked to confirm that the member is indeed a deep beam so that ACI 318, Appendix A, can be used for design. If the member is considered a deep beam, node locations should be determined for the tension tie. The nodes should be approximately $a/2$ from the bottom of the beam. A good estimate for this location is $0.05h$ or approximately 5 inches (MacGregor & Wight, 2005).

3.4.1 Struts

Node locations should be determined for the tension tie. The nodes should be approximately $a/2$ from the bottom of the beam.

$$F_{ns} = f_{ce} A_{sc}$$

Where:

A_{sc} = X-sectional area of the strut at one end;

f_{ce} = compressive strength of concrete.

The compressive strength of concrete in the strut is calculated by using ACI 318-11; Equation A-3 in Appendix-A. The strength of the nodal zone is calculated by using Equation A-8, as given below, respectively.

$$f_{ce} = 0.85\beta_s f'_c$$

$$f_{ce} = 0.85\beta_n f'_c$$

where:

β_s = factor to consider the cracking effect;

β_n = factor to consider the anchorage effect of ties.

According to ACI 318-11, Section A.3.2.1, for a uniform cross-section area over the length of the strut, $\beta_s=1.0$ which indicates that the strut has an equivalent stress block of depth “a” and a width “b” identical to beams (MacGregor & Wight, 2005).

ACI 318-11, Sections A.3.2.3 gives the value $\beta_s=0.40$ for struts in tension members or tension flanges. Concrete is not good in tension, so the tension force will cause cracks to pull apart thus greatly decreasing the strength of the strut. Section A.3.2.4 gives the value of $\beta_s = 0.60$ for all other situations not mentioned in the previous sections.

If a strut does not have enough strength, compression reinforcement can be added much like a column that includes longitudinal reinforcement along the axis of the strut with ties or spiral reinforcement in accordance with ACI 318-11, Section 7.10. ACI 318-11 Equation A-5, is used to determine the compressive strength of a longitudinally reinforced strut.

$$F_{ns} = f_{ce}A_{cs} + A_s f_s'$$

Where:

A_{cs} = cross sectional area at one end of a strut normal to the axis of the strut;

A_s' = area of compression reinforcement;

f_s' = stress in compression reinforcement under factored loads.

3.4.2 Nodal Zones

Nodal zones are designed assuming that they will fail by crushing (MacGregor & Wight, 2005). ACI 318-11, Equation A-7, sets the limit of the nominal compressive strength of a nodal zone, F_{nn} . As in Section 4.6.1, the concrete compressive strength of the node is calculated by using ACI 318-11 Equation A-8.

$$F_{nn} = f_{ce}A_{nz}$$

$$f_{ce} = 0.85\beta_n f'_c$$

Where:

A_{nz} = smaller of (a) that area of the nodal zone which is perpendicular to the line of action and on which F_u is applied, or (b) that area of the nodal zone which is perpendicular to the line of action and on which resultant force is applied.

ACI 318-11, Section A.5.2 gives values for β_n based on the geometry of the nodal region. If the nodal zone is bounded by compressive struts, C-C-C, $\beta_n = 1.0$. If the nodal zone is bounded by compressive struts with one tension tie, C-C-T, $\beta_n = 0.80$; and if the nodal zone is bounded by two or more tension ties, C-T-T or T-T-T, $\beta_n = 0.60$. Tension ties decrease nodal strengths because of the increased disruption due to the incompatibility of tension strains and compressive strains (ACI Committee 318, 2008). However, tests have shown that C-C-T and C-T-T nodes develop $\beta_n = 0.95$ when properly constructed (MacGregor & Wight, 2005). The values selected are conservative and allow for construction tolerances.

3.4.3 Ties

Reinforcement is used in ties to tackle the tension in the element which is to be designed and tension in the surrounding concrete. Although the concrete increases the axial stiffness of the tie through tension stiffening but takes no contribution in the resistance of forces. The ACI 318-11 Equation A-6 is used for the determination of the strength of the tie.

$$F_{nt} = A_{ts}f_y + A_{tp}(f_{se} + \Delta f_p)$$

Where:

$$(f_{se} + \Delta f_p) \leq f_y \text{ and } A_{tp} \text{ is 0 for non-pre-stressed members.}$$

The limit of the effective width, w_t , of the tie depends on the distribution and geometry of the reinforcement. The axis of the tie and the axis of the reinforcement in the tie shall coincide with each other as per the provisions of ACI-318, Section A.4.2 and RA.4.2. In case of one layer of bars, the lower limit for w_t is the diameter of the bar plus twice the concrete cover. For the upper limit of w_t , the following equation is used:

$$w_{t,max} = \frac{F_{nt}}{f_{cu}b}$$

3.5 Results and Discussion

The principal stresses occur at a plane at which shear stress components become zero. From design point of view, maximum normal stresses are determined which are induced at a given point. There is one plane i.e. principal plane (more precisely maximum principal plane) on which normal stress is maximum and normal stress on this plane is principal stress (more precisely maximum principal stress). In SAP2000, the maximum principal stresses are denoted by S_{Max} . If the value of the maximum principal stress is more than $7.5\sqrt{f_c'}$ (psi) as per the provisions of ACI-318, then cracking in the cover concrete must be developed in the RCC member.

The comparison of concrete tensile strength and maximum principal stresses can be used for the determination of crack pattern in concrete. As per ACI-318, the tensile strength of concrete is $7.5\sqrt{f_c'}$ (psi). In this case, the compressive strength of concrete is 6000 psi so the tensile strength is 580 psi.

The cracks pattern of the non-linear shell layered model was compared with the experimental results available in literature. The crack pattern of non-linear shell layered model was found resembling with those observed in previous experimental researches (Bircher et al. 2009 and Masab et al. 2014), as shown in Figure 3.4.

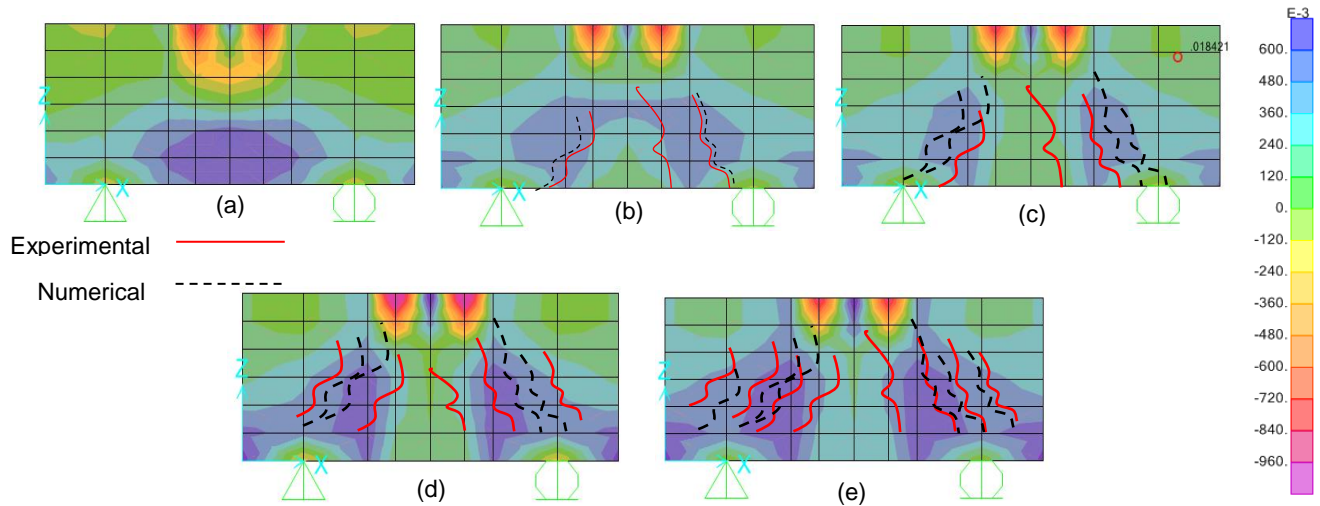


Figure 3.4. Cracking pattern of prototype beam (non-linear shell layered element) at a load of; (a) 30Kips, (b) 47Kips, (c) 78Kips, (d) 94Kips and (e) 109Kips

Using the comparison of concrete tensile strength and maximum principal stresses, the behavior of prototype beam sample by the non-linear shell layered element is shown in Figure 3.4. To get a clear view of the behavior, the cracks have been shown by drawing lines at cracks location. The solid lines are the representation of the cracks as observed in the previous studies by Birrcher et al. 2009 and Masab et al. 2014. The dashed lines represent the cracks pattern found numerically i.e. the regions where the normal stress is more than that of 580psi.

At a load of 30 kips, no cracks are found i.e. the principal stress (in case of non-linear shell layered model) is less than 580 psi confirming no cracks in beam specimen as shown in Figure 3.4(a). The first flexural crack is observed at the bottom of the beam at a load of 47 kips i.e. the principal stress is almost 3% more than 580 psi which confirms the initiation of crack as shown in Figure 3.4(b). At a load of 78 kips, the value of principal stresses increased up to 17% from 580 psi confirming the extension of crack length as shown in Figure 3.4(c). At a load of 94 kips, the cracks are observed at both supports as well and the principal stress is 37% more than 580 psi as shown in Figure 3.4(d). At a load of 109 kips, the value of principal stress is almost 57% more than that of 580 psi at most of the beam section as shown in Figure 3.4(e). The crushing of concrete does not occur. The behavior of bottom, top and transverse reinforcement at a load of 94kips is shown in Figure 3.5.

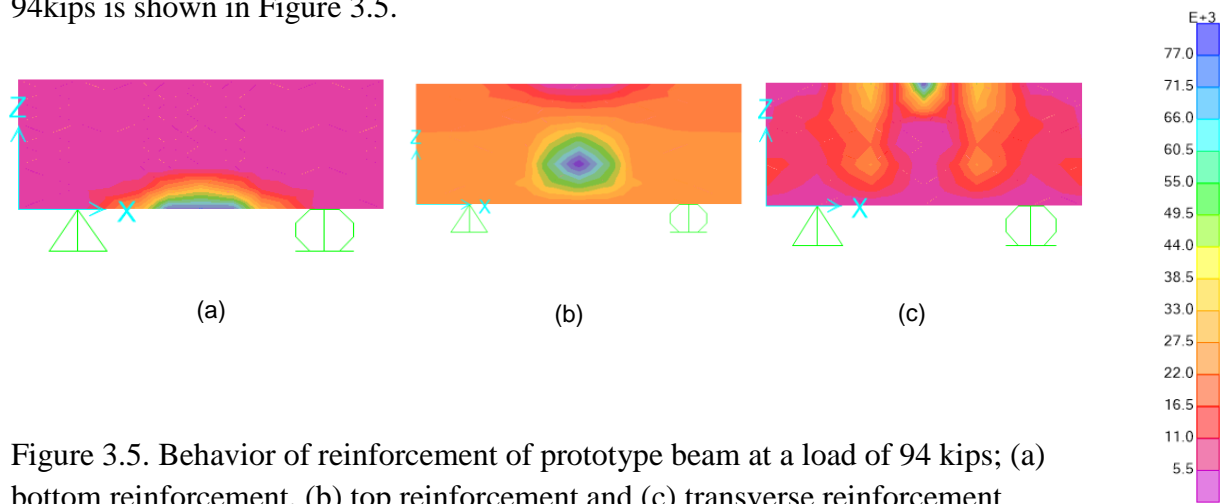


Figure 3.5. Behavior of reinforcement of prototype beam at a load of 94 kips; (a) bottom reinforcement, (b) top reinforcement and (c) transverse reinforcement

Stresses
in psi

At a load of 94Kips, the bottom reinforcement stress reached up to 96% of its yield strength and the top reinforcement stress reached up to 91% of its yield strength. The shear/transverse reinforcement stress reached up to 96% of its yield strength.

The behavior of bottom, top and transverse reinforcement at a load of 109kips is shown in Figure 3.6.

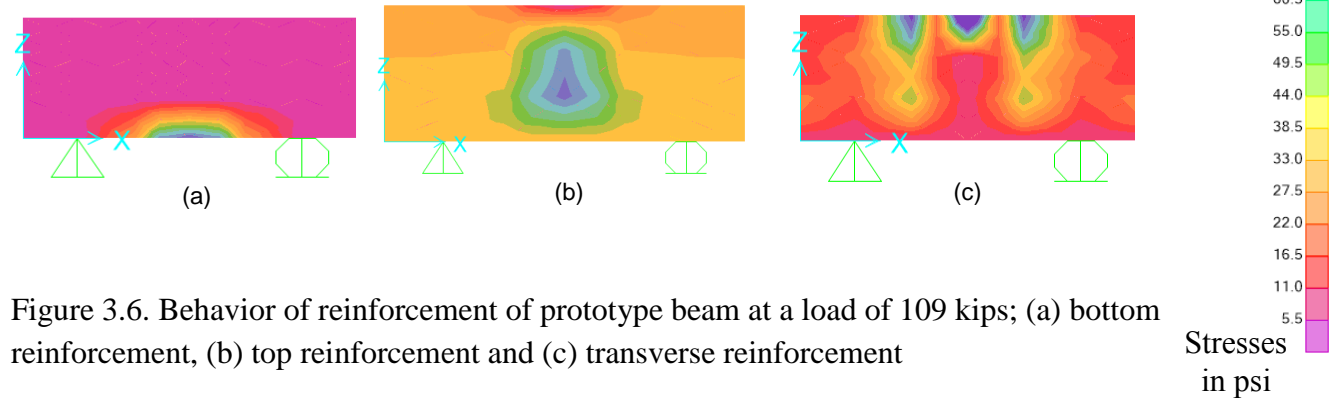


Figure 3.6. Behavior of reinforcement of prototype beam at a load of 109 kips; (a) bottom reinforcement, (b) top reinforcement and (c) transverse reinforcement

At a load of 109kips, the bottom reinforcement stress, shear/transverse reinforcement stress and top reinforcement stress exceeded the yield strength by 14%, 50% and 10%, respectively, which confirms the yielding of steel reinforcement

Model	Strain Distribution Diagram
Non-linear shell layered	
Niranjan and Patel (2012)	

Table 3.1. Qualitatively comparison of strain distribution diagram of non-linear shell layered element with experimental diagram in literature

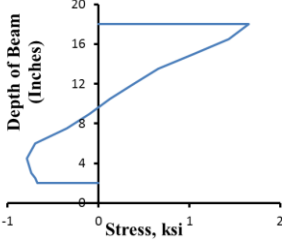
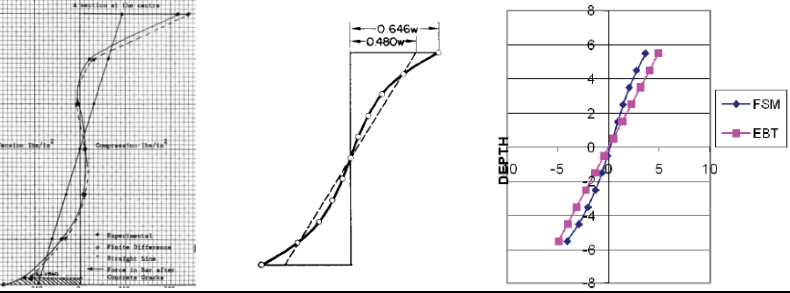
Model	Stress Distribution Diagram
Non-linear shell layered	
Niranjan and Patel (2012)	

Table 3.2. Qualitatively comparison of stress distribution diagram of non-linear shell layered element with experimental diagrams in literature

The strain distribution along the depth of the small prototype beam for non-linear shell layered modeling technique is shown in Table 3.1. As can be seen that the strain distribution is non-linear. Similar distribution was observed in the experimental study performed by Niranjan and Patil (2012). The strain distribution of the reference non-linear shell layered model resembles well with the strain distribution available in the literature.

The stress distribution of small prototype beam for non-linear shell layered modeling technique is shown in Table 3.2. As can be seen that the stress distribution is non-linear. Similar distribution was observed in the experimental study performed by Holmes et al. (1972), Aftab (1965) and Niranjan and Patil (2012). The stress distribution of the reference non-linear shell layered model resembles well with the stress distribution available in the literature.

On the basis of the similarity of experimental results with that of non-linear shell layered model, the non-linear shell layered model amongst the modeling techniques mentioned in the previous sections is taken as a reference for further investigation.

The maximum deflection at mid-point is also determined for small prototype beam using non-linear shell layered model for a load of 109kips as shown in Figure 3.7 (dotted line). To approximately align all other models in respect of mid span deflection to that of non-linear shell layered model, modification factors are changed by hit and trial method.

Model	Factors Before Alignment			Factors After Alignment		
	I	E	G	I	E	G
Non-linear shell layered	1.0	1.0	1.0	0.35	1.0	1.0
Frame/Line	0.35	1.0	1.0	1.0	0.20	0.20
Shell/Area	0.35	1.0	1.0	0.35	1.0	1.0
Solid/3D	1.0	1.0	1.0	1.0	0.40	0.40
STM	0.35	1.0	1.0	1.0	1.0	1.0

Table 3.3. Suitable modification factors

Table 3.1 summarizes the modification factors before and after the alignment of other models to that of non-linear shell layered model. After accounting for the cracking effects, the mid-point deflection from different modeling technique is also shown Figure 3.7. It can be seen that the deflection obtained from all modeling technique after modification is almost the same (dashed line).

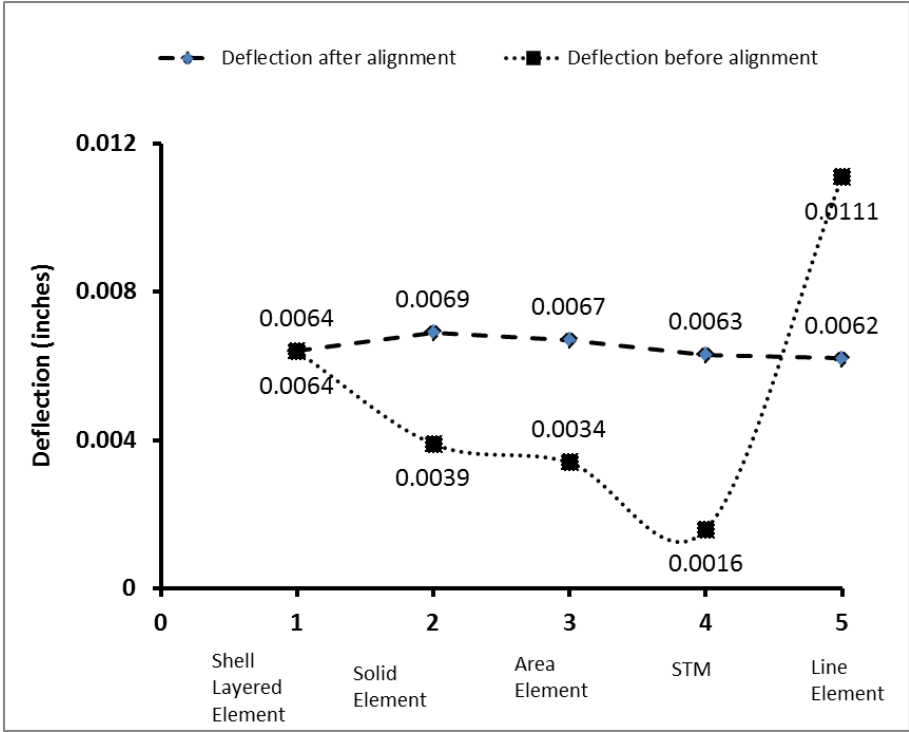


Figure 3.7. Deflection of small prototype beam before and after the alignment of other models compared to that of non-linear shell layered model

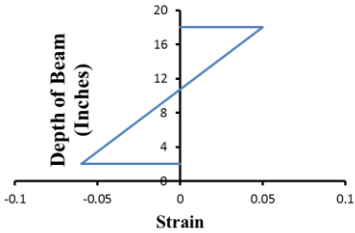
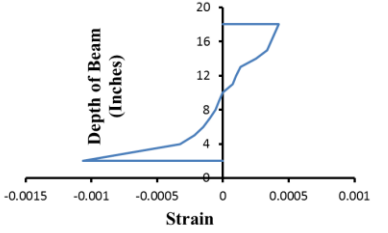
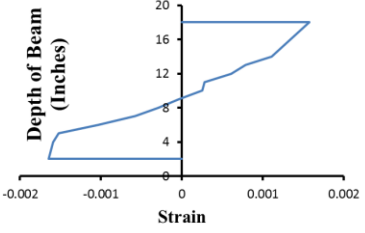
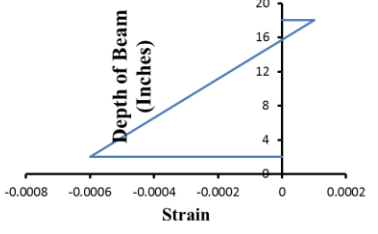
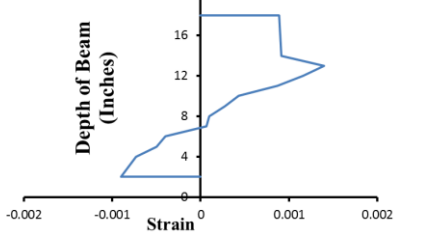
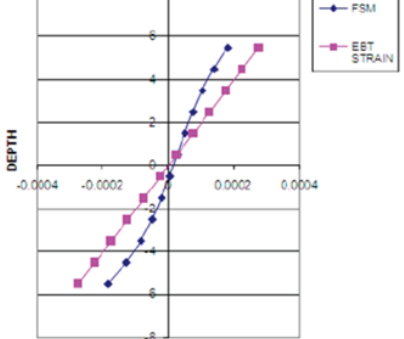
Model	Strain Distribution Diagram
Frame/line	
Shell/area	
Solid/3D	
STM	
Non-linear shell layered	
Niranjan and Patel (2012)	

Table 3.4. Strain distribution diagrams for different modeling techniques

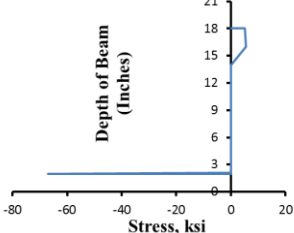
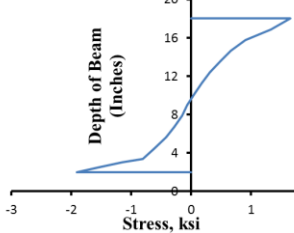
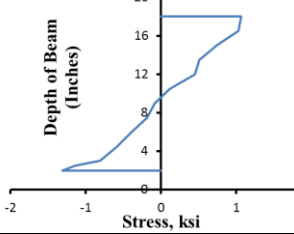
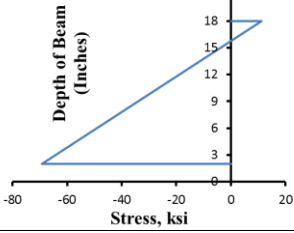
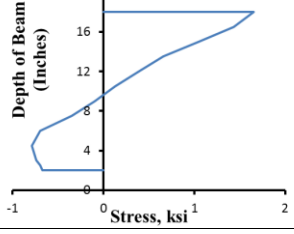
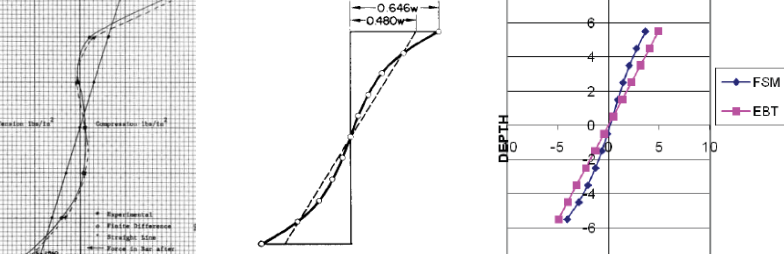
Model	Stress Distribution Diagram
Frame/line	
Shell/area	
Solid/3D	
STM	
Non-linear shell layered	
Aftab (1965) Holmes (1972) Niranjan and Patel (2012)	

Table 3.5. Stress distribution diagrams for different modeling techniques

The strain distribution along the depth of the small prototype beam for shell/area, solid/3D element and non-linear shell layered modeling technique is shown in Table 3.4. The beam except line and STM, is divided into number of elements along the length. These elements are further divided into five horizontal layers. The change in length (found by change in displacement at two adjacent points) divided by the original length for each horizontal layer i.e. strain is found between two points along the depth under the load (magnitude of 109kips). The strain distribution diagrams are drawn along the depth. In case of line element, the section designer utility of SAP2000 is used, where the strain distribution diagram at the desired moment can easily be obtained. In case of STM the strain under axial force (magnitude of 109kips) is found at bottom and top the TG and drawn along the depth of the beam. As can be seen that the strain distribution is non-linear for all models except line and STM. Similar distribution was observed in the experimental study performed by Niranjana and Patil (2012). The strain distribution of the reference non-linear shell layered model resembles well with the stress distribution available in the literature. The strain distribution from the solid element model is matching well with that obtained from the reference non-linear shell layered element model.

The stress distribution of small prototype beam for shell/area, solid/3D element and non-linear shell layered modeling technique is shown in Table 3.5. Just like in strain distribution diagrams, the beam except line and STM is divided into number of elements along the length. These elements are further divided into five horizontal layers. The stress at a load of 109kips is found between two points along the depth. When sufficient data obtained, the stress distribution diagrams are drawn along the depth. In case of line element the section designer utility of SAP2000 is used, where the axial force at the desired moment can easily be obtained. The force (compression in case of concrete and tension in case of steel) is divided by area i.e. concrete area at the top for compressive stress and steel area for tensile stress at the bottom. In case of STM the axial force is found at bottom and top the TG. The force is divided by the area of strut for compressive stress and by the area of steel tie for tensile stress, and drawn along the depth of the beam. As the tensile stress is much more as compared to concrete compressive stress therefore the original value of concrete stress for line element and STM is multiplied by 10 for the purpose of presentation. As can be seen that the stress distribution is non-linear. Similar distribution was observed in the experimental study performed by Holmes et al. (1972), Aftab (1965) and Niranjana and Patil (2012). The stress distribution of the reference non-linear shell layered model

resembles well with the stress distribution available in the literature. Like the strain distribution, the stress distribution from the solid element model is matching well with that obtained from the reference non-linear shell layered element model.

3.6 Summary of Prototype Beam

The summary of small prototype beam is as follows:

- The beam sample is designed using STM technique of ACI-318.
- The beam is then modeled using different modeling techniques available in commercially available software's.
- Total 25 numbers of simulations are carried out in case of small prototype beam. These different modeling techniques are compared to each other in respect of different parameters.
- Some basic details regarding different modeling techniques i.e. frame/line element, shell/area element, solid/3D element, non-linear shell layered element and STM, are also provided.
- The cracks pattern and stress and strain distribution of non-linear shell layered model is compared to that of experimental findings available in the literature. It is observed that the results obtained from non-linear shell layered modeling technique are qualitatively matching well with experimental studies.
- On the basis of this resemblance with experimental findings, the non-linear shell layered modeling technique is taken as a reference model for recommendations to other models.
- The rest of the modeling techniques are compared to that of reference modeling technique. The maximum deflection is different for different modeling techniques. All the models are approximately aligned to the reference model in respect of maximum deflection at mid span, and for this purpose different modification factors are set by hit and trail.
- At a load of 94Kips, the bottom reinforcement stress reached up to 96% of its yield strength and the top reinforcement stress reached up to 91% of its yield strength. The shear/transverse reinforcement stress reached up to 96% of its yield strength.

- At a load of 109kips, the bottom reinforcement stress, shear/transverse reinforcement stress and top reinforcement stress exceeded the yield strength by 14%, 50% and 10%, respectively, which confirms the yielding of steel reinforcement.

CHAPTER 4 CASE STUDY

4.1 Introduction

A small prototype beam as discussed in previous chapter was studied for the suitable modeling technique and stiffness modification factors for transfer girders. To assess the true gravity and seismic forces in reinforced cement concrete (RCC) structures, the results of small prototype beam were compared to that of experimental findings available in literature. In this chapter, the concept and findings from small prototype beam are extended to 11-storied RCC frame structure. This chapter focuses on the detailed discussion of case study structure, different modeling techniques, response spectrum analysis (RSA) and equivalent static analysis (ESA). Different parameters e.g. storey drift, storey shears and overturning moment etc., are compared from each modeling technique and on the basis of the results obtained, best modeling technique is recommended.

4.2 Description of Case Study Structure

The elevation and 3D view of a typical 11-storied building (Three Basements, Ground Floor+ Seven Floors) taken as a case study is shown in Figure 4.1. Typical storey height is 12 feet. The soil condition beneath and surrounding the building is represented by stiff clayey soil. This is equivalent to the soil profile type SD in the UBC-97 (1997). The plane dimensions of the building in the basement floors are 150 feet length x 100 feet width up to Ground Floor. An offset of 20 feet in short direction and 25 feet in long direction from both sides has been given to the floors above the ground. Thus plane dimensions in the upper floors are 100 feet length x 60 feet widths. The first three basements are to be used for the parking; the ground and 1st for commercial shops, 2nd and 3rd for offices and the remaining stories are for residential purposes. Typical planes at different levels are shown in Figure 4.3. In the first three levels, the grid spacing is 33.34 ft in x-direction and 30 ft in y-direction. In the upper levels, the grid spacing is 20 ft in X-direction and 25 ft in Y-direction. As the grid spacing changes in the ground floor, therefore a transfer structure (transfer girder) has to be introduced at this level to act as a “so called foundation” for the columns above ground floor. In this specific case, four (04) numbers of TG are used in long and short directions, as shown in Figure 4.1. The depth of the TG is taken

as 5 feet keeping in view the span of 33.34 feet and loading from the columns above. Transfer girders are modeled using different modeling techniques discussed in previous chapter.

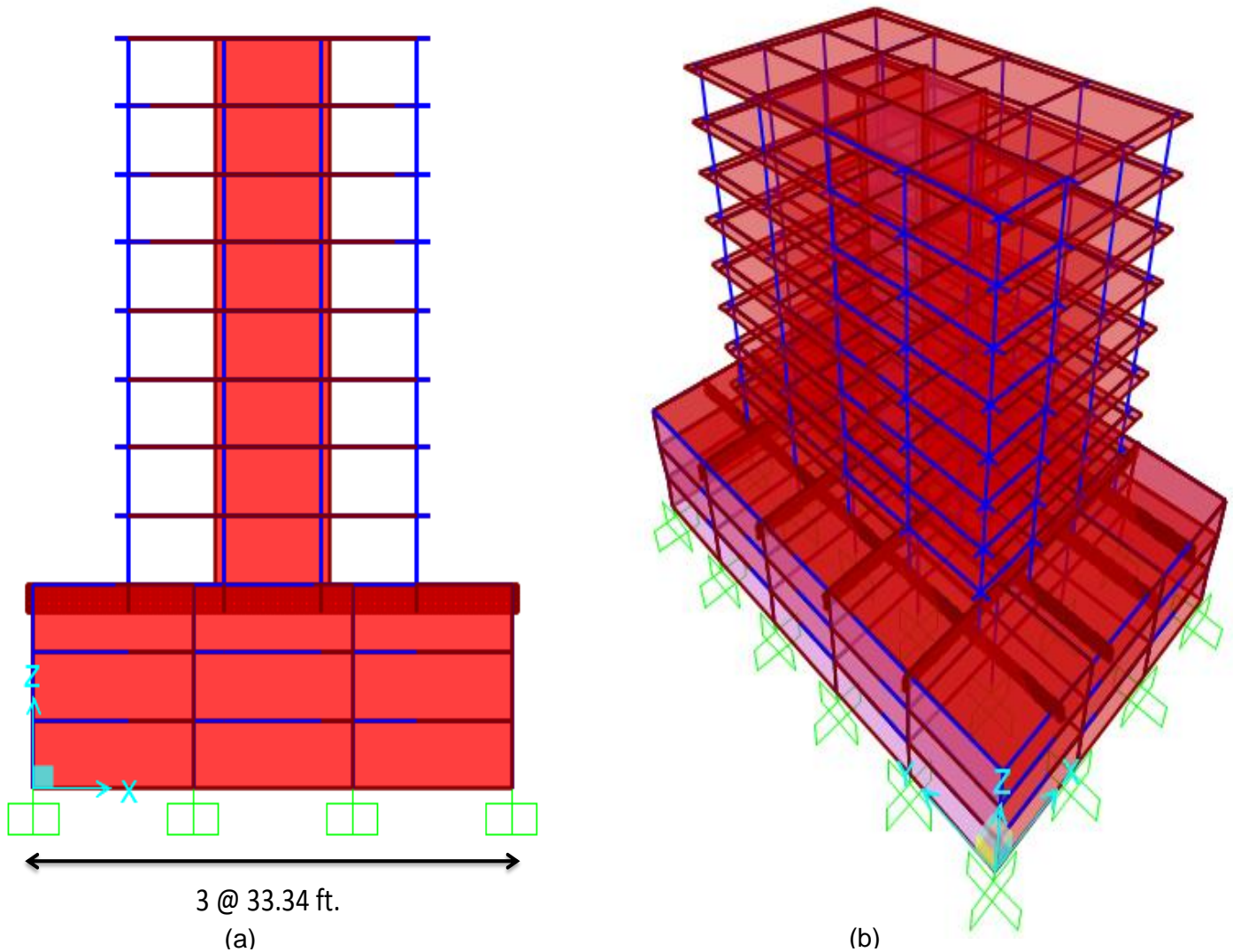


Figure 4.1. (a) XZ-Elevation and (b) 3D view of the case study building

The case study structure is analyzed using UBC-97 design code for seismic zone-4 and soil profile type SD for 5% damping in each and every mode. UBC-97 is used since it has been widely used as a model code for seismic design of buildings in many countries. Different load combinations taken from UBC-97 are used. The load combinations of 1.4 (dead load) and 1.2 (dead load) + 0.5 (live load) + 1.0 (earthquake load) are used as a gravity load and gravity plus seismic loading, respectively. The building is analyzed in both X and Y-directions. The commercial Computer Structure International (CSI) software SAP2000 (V15) is used for

analysis. All the longitudinal, transverse, and mid depth bars details, which shall be used later on in non-linear shell model, are worked out by modeling and designing TGs as line element according to ACI-318-11. One cross section of the TG is shown in Figure 4.2. The bending moment at the bottom of the TG is 1280 kip-ft., for this bending moment, the area of steel calculated is 5.34 in². Therefore, 7#8 bars are used. The rest of the TGs are designed using the same procedure.

Please note that the stiffness modification factors for line element worked out for small prototype beam are used.

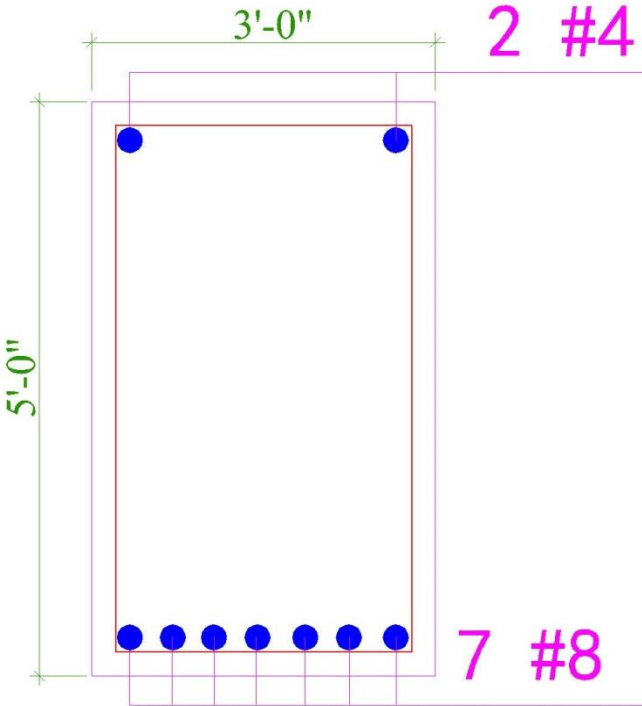
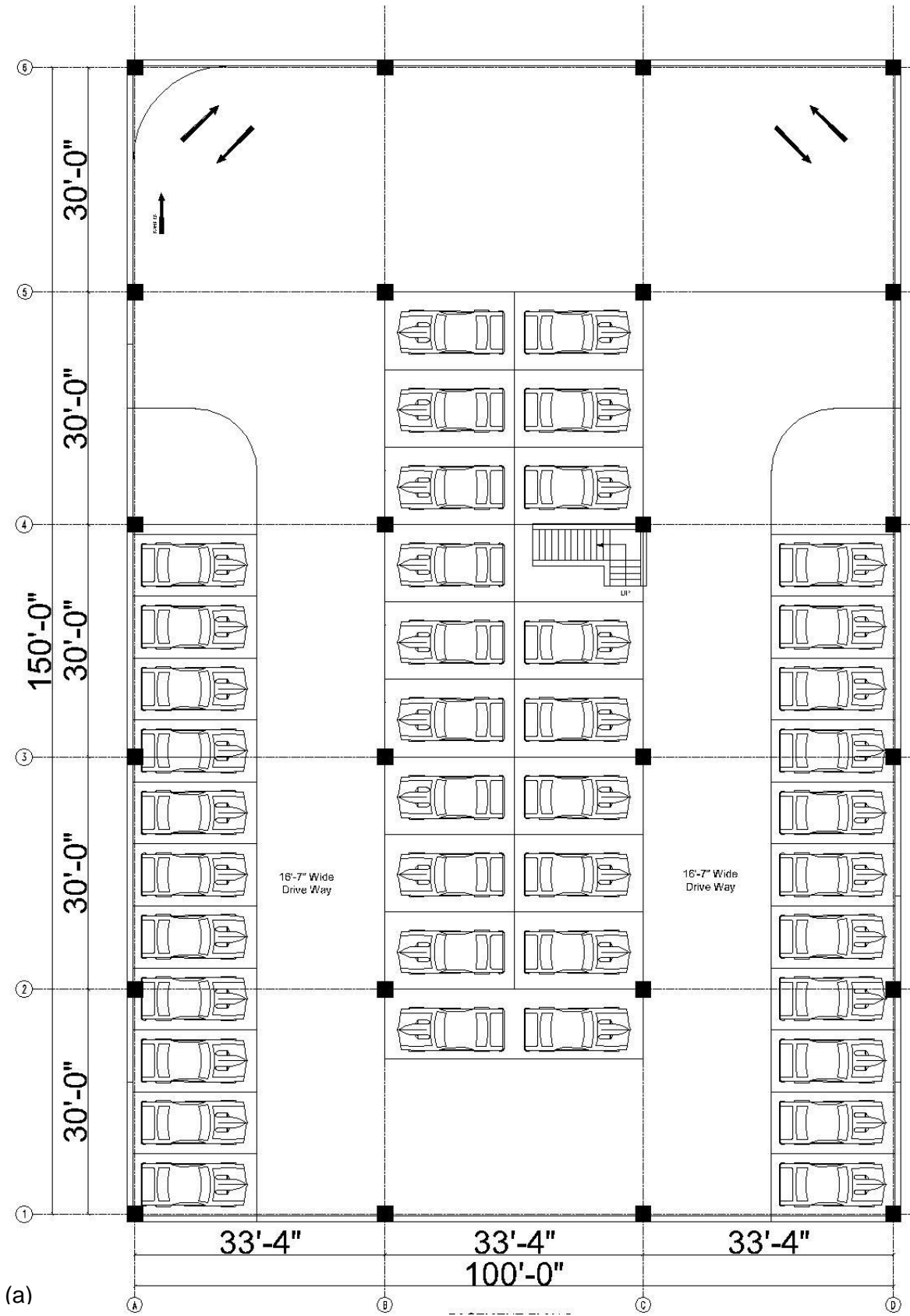
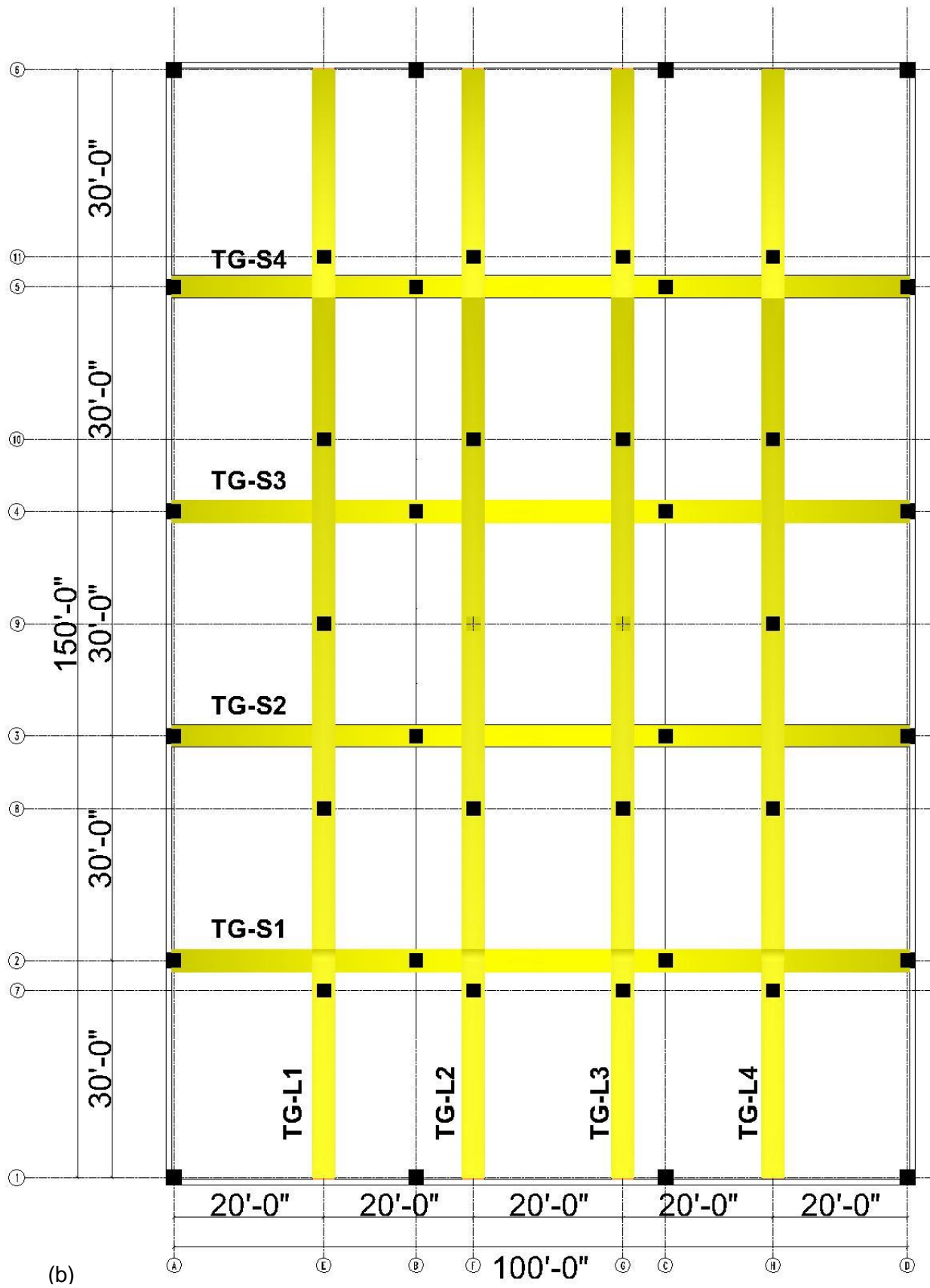
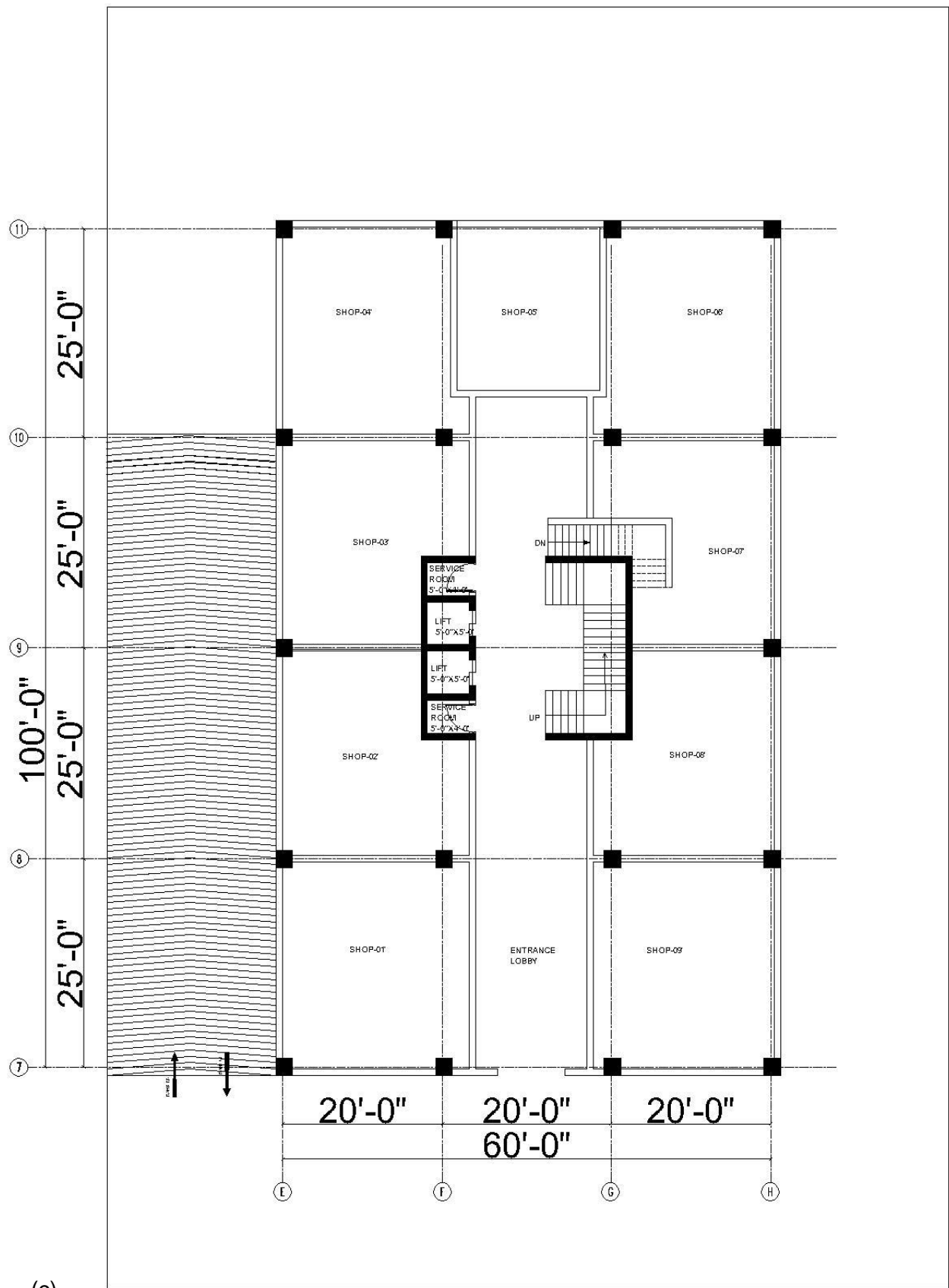


Figure 4.2. X-section of a TG







(c)

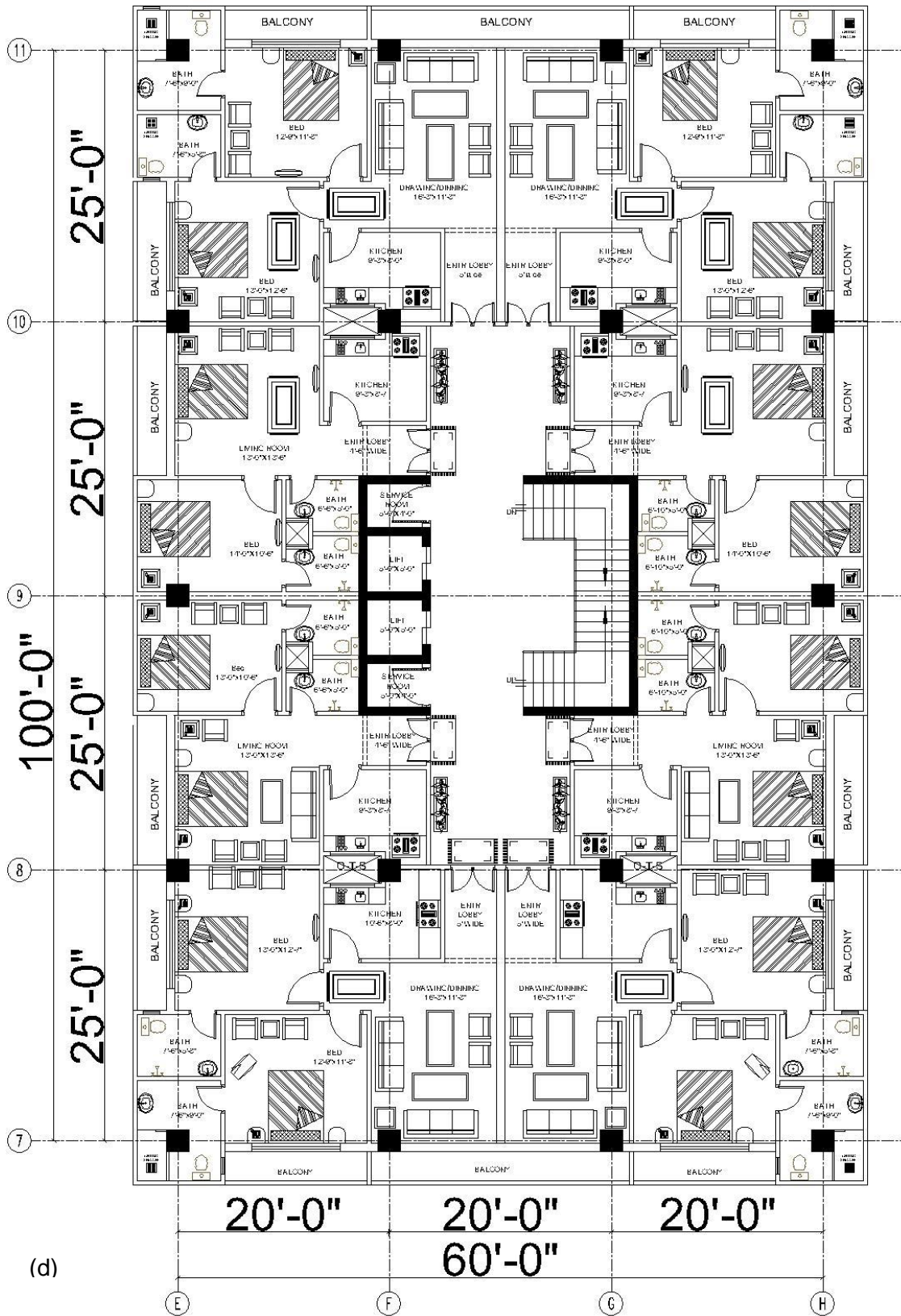


Figure 4.3. Architectural plans: (a) Typ. basement plan, (b) TGs layout (c) Typ. ground floor plan and (d) Typical apartments plan

The TG's are then modeled using different modeling techniques presented in previous chapter, as shown in Figure 4.4. The non-linear shell layered element is considered as a reference to which the results of other techniques are compared. The modifications factors are kept the same as those used for modeling of prototype beam after the alignment of other models to that of non-linear shell layered model in respect of mid-span deflection. In this case, the compressive strength of concrete is 3750 psi, therefore the tensile strength is 460 psi according to ACI-318 formula for tensile strength ($7.5\sqrt{f_c}$ (psi)). The deep girder is divided into 1ft square elements, in both directions in case of shell/area, solid/3D and non-linear shell layered models. One TG in X-direction on which the core wall rests, is checked for cracks and maximum deflection. Furthermore, the non-linear shell layered model is also checked for yielding of bottom, top and shear reinforcement and also for maximum strain.

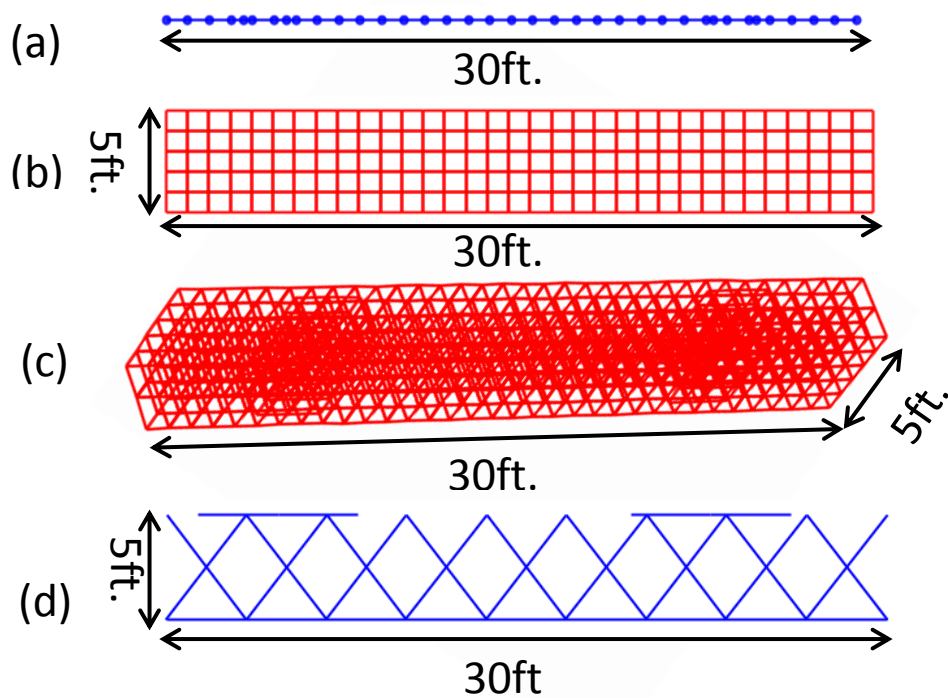


Figure 4.4. Different modeling techniques of TG of case study structure (a) frame/line element, (b) thick shell/area element and non-linear shell layered element, (c) solid/3D element and (d) STM

4.3 Equivalent Static Analysis (ESA)

The existing nonlinear approaches are of great accuracy for evaluation and estimation of seismic demands, but the complexities involved in developing the model, are not generally addressed. The equivalent static analysis is one of the common approaches used for seismic demand analysis of structures, which is deemed as one of the fastest and most practical methods in most codes. This procedure is used for common structures (residential buildings with moderate height). The indication of the strengths on the structure is necessary for the earthquake resistant design of a structure. The actual forces which can happen over the whole life of the structure cannot be predicted accurately. As the development and maintenance cost of the structure ultimately depends upon the safe and economical design of the structure, so a practical measurement of these forces is critical in any case. Many factors are related to the application of seismic forces on the structure like magnitude of earthquake, distance of fault from the structure, geology of the site and lateral load resisting mechanism of the structure.

Two methods are commonly used for the specification of seismic design forces: "Equivalent Static Force Procedure" and "Dynamic Analysis". In case of equivalent static force procedure, the forces due to inertia are taken as static forces using numerical relations. The analytical relationships do not clearly consider the "dynamic characteristics" for the specific structure which is analyzed or designed. The structures which have a reasonably uniform distribution of mass and stiffness are called regular structures. For the effective consideration of dynamic behavior of such type of structures, many analytical relationships are developed. The equivalent static force procedure is most often suitable in case of regular structures. The other category is of irregular structures. In such type of structures, large floor to floor variation in mass or center of mass and soft stories are the general irregularities. These types of structures do not fit as per the assumptions used in the empirical relationship, utilized in the equivalent static force procedure.

Equivalent static force procedure or a dynamic analysis is suitable for 240 feet tall in case of regular structures and 65 feet tall in case of irregular structures as per the provisions by UBC-97. When the structure height exceeds the limit of 240 feet in case of regular structures, 65 feet in case of irregular structures and in case of buildings which are located on soil type-SF and having a time period more than 0.7 seconds, dynamic analysis response spectrum is required.

4.4 Response Spectrum Analysis (RSA)

The quantification of the structure's response to the complex ground motions is the basis for the need of engineering seismology. The structure's mass and stiffness distribution determines the response of the structure. For example, low acceleration relative to the ground is experienced by stiff buildings. Tall structures have a tendency to accelerate far from ground movements, bringing about low accelerations. In-homogeneity inside the building may bring about twisting (Silva 2005).

Italian engineers started handling the issue of seismic response structural design after the 1908 Reggio Calabria quake, which, in conjunction with a torrent, guaranteed almost 100,000 lives. They utilized a static approach.

Before the twentieth century, the concept of "response spectrum" was not in use in earthquake engineering. In the mid twentieth century, the concept of the "response spectrum" was applied in design requirements. The widespread use came into existence in 1970s in earthquake engineering when strong-motion accelerograph data became widely available (Trifunac and Todorovska, 2008).

For the evaluation of the given structure's behavior, earthquake acceleration records can be applied to a mathematical model of a building, e.g. with known masses, stiffness values and dimensions for each level (Clough, 1962). Linear superposition of single degree of freedom systems for different modes and respective natural frequencies represents the system's response (Trifunac and Todorovska, 2008).

The case study structure is modeled using different modeling techniques. The response spectrum analysis (RSA) and equivalent static analysis (ESA) are also used as a seismic analysis tools. Different parameters e.g. cracks pattern, maximum deflection, storey drift ratios, storey shears, overturning moment, strain and stress distribution are compared from each modeling technique and on the basis of the results obtained, best modeling technique is recommended.

The results obtained from ESA and RSA are found comparable as shown in the Figure 4.10 and 4.12. This is because of the fact that the case study structure is a regular structure and its height

is less than less than 240 ft. Therefore, the results obtained from ESA are used for further investigation in Section 4.6.

4.5 Results and Discussion

4.5.1 Behavior of the TG using non-linear shell layered model based on ESA

It is prudent to discuss the behavior of the TG and superstructure for case of non-linear shell layered model being the reference model. The time period of the structure using non-linear shell layered modeling is 0.820 seconds in first mode. The participation of the first mode is 84% i.e., this building is dominated by the 1st mode. The crack pattern of non-linear shell layered model is observed by comparing the concrete tensile strength and principal stresses as done for small prototype beam. To get a clear view of cracks in TG, cracks are shown by drawing lines in each figure. In non-linear shell layered element model, the maximum stresses are observed in TG below the core wall of ground floor. Under gravity loading, the principal stress is almost 20% more than that of 460 psi at the bottom of TG which means that the cracks may be developed at the bottom of TG, as shown in Figure 4.5(a). Under gravity plus seismic loading, the principal stress is almost 39% more than that of 460psi below the core wall and at right side of the core wall as shown in Figure 4.5(b), which means that the cracks width may be increased. The bottom reinforcement stress reached up to 13% of its yielding strength under gravity loading and up to 33% under gravity plus seismic loading as shown in Figures 4.5(c) & (d). The top reinforcement stress reached up to 9% of its yielding strength under gravity loading and up to 27% under gravity plus seismic loading as shown in Figures 4.5(e) & (f). The shear reinforcement stress reached up to 5% of its yielding strength under gravity loading and up to 22% under gravity plus seismic loading as shown in Figures 4.5(g) & (h). The concrete reached up to 20% of its maximum strain.

Maximum deflections at mid span under core wall obtained from the analyses of deep girders using different modeling techniques are shown in Figure 4.6. The minimum deflection of 0.1834 inches is obtained in case of non-linear shell layered model. Moreover, the storey shears, overturning moments and storey drift ratios are determined for non-linear shell layered model also.

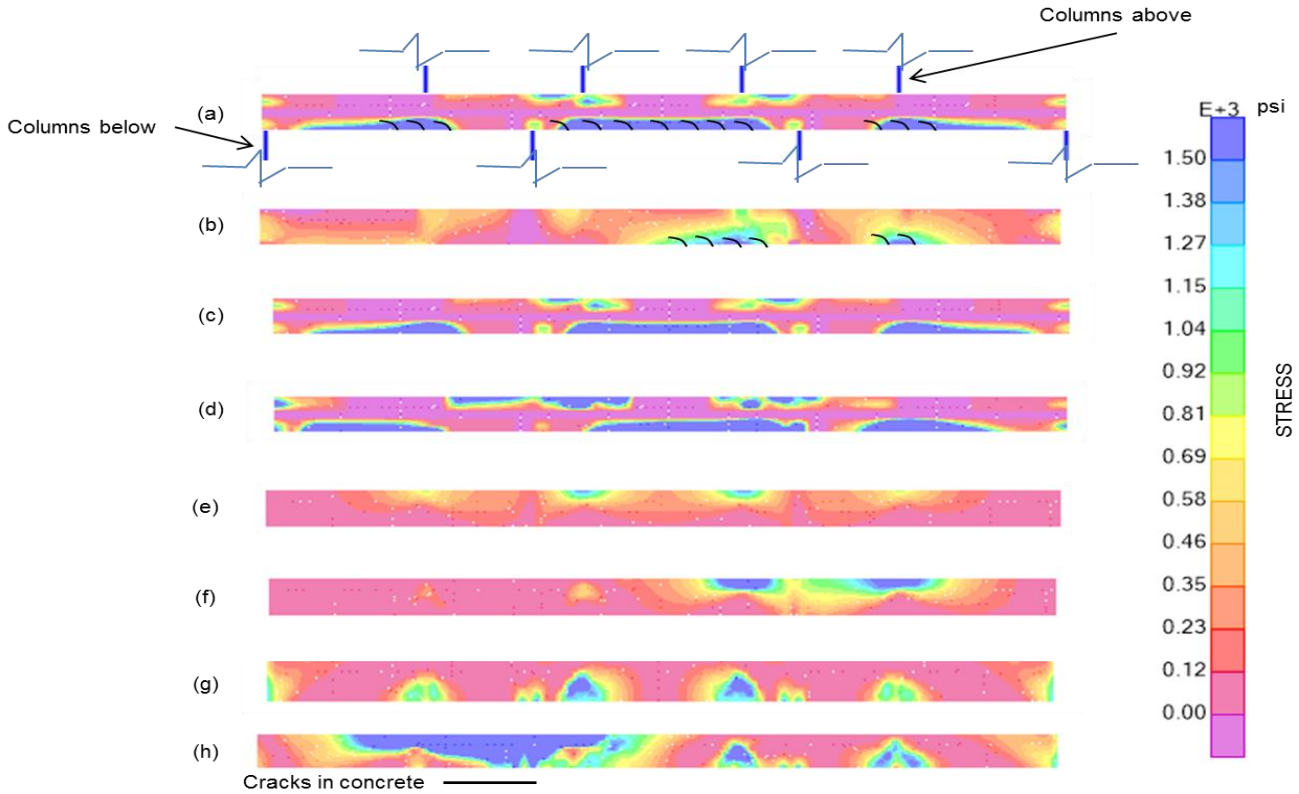
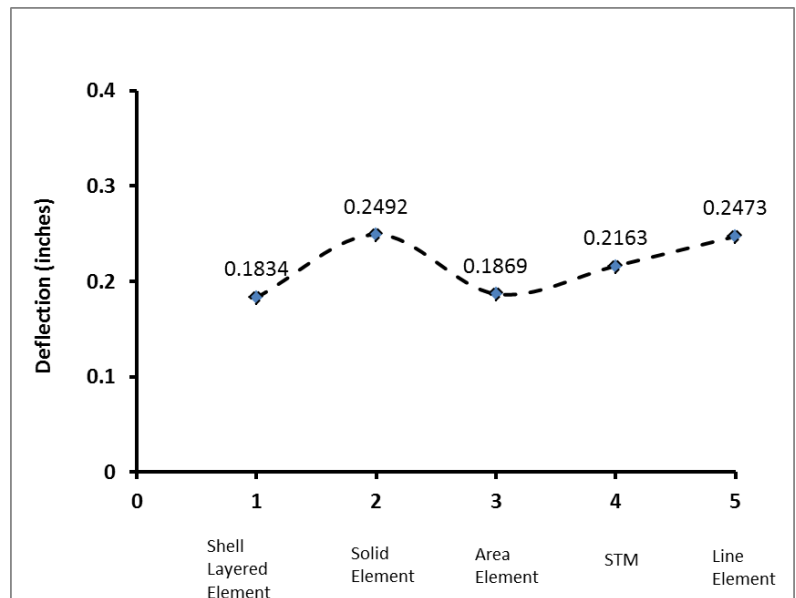


Figure 4.5. Behavior of TG from non-linear shell layered element; (a) crack pattern under factored gravity loading, (b) crack pattern under gravity plus seismic loading, (c) bottom reinforcement under gravity loading, (d) bottom reinforcement under gravity plus seismic loading, (e) top reinforcement under gravity loading, (f) top reinforcement under gravity plus seismic loading, (g) shear reinforcement under gravity loading, (h) shear reinforcement under gravity plus seismic loading

Figure 4.6. Maximum deflection of TG from different modeling techniques



The non-linear shell layered model among the available modeling techniques is taken as a reference as its behavior was found resembling with the experimental observations in prototype beam as discussed in Chapter 03. The comparison of non-linear shell layered model with that of other models is presented below.

4.5.2 Comparison of non-linear shell layered model with other models

The time period for frame/line model, shell/area model, solid/3D model and STM is 0.895, 0.810, 0.812 and 0.845 seconds respectively. It may be noted that the time period of line model and STM is 8% and 3%, respectively, more than that of non-linear shell layered model. The time periods of shell/area and solid/3D model are 1.2% and 0.03% less than that of non-linear shell layered model.

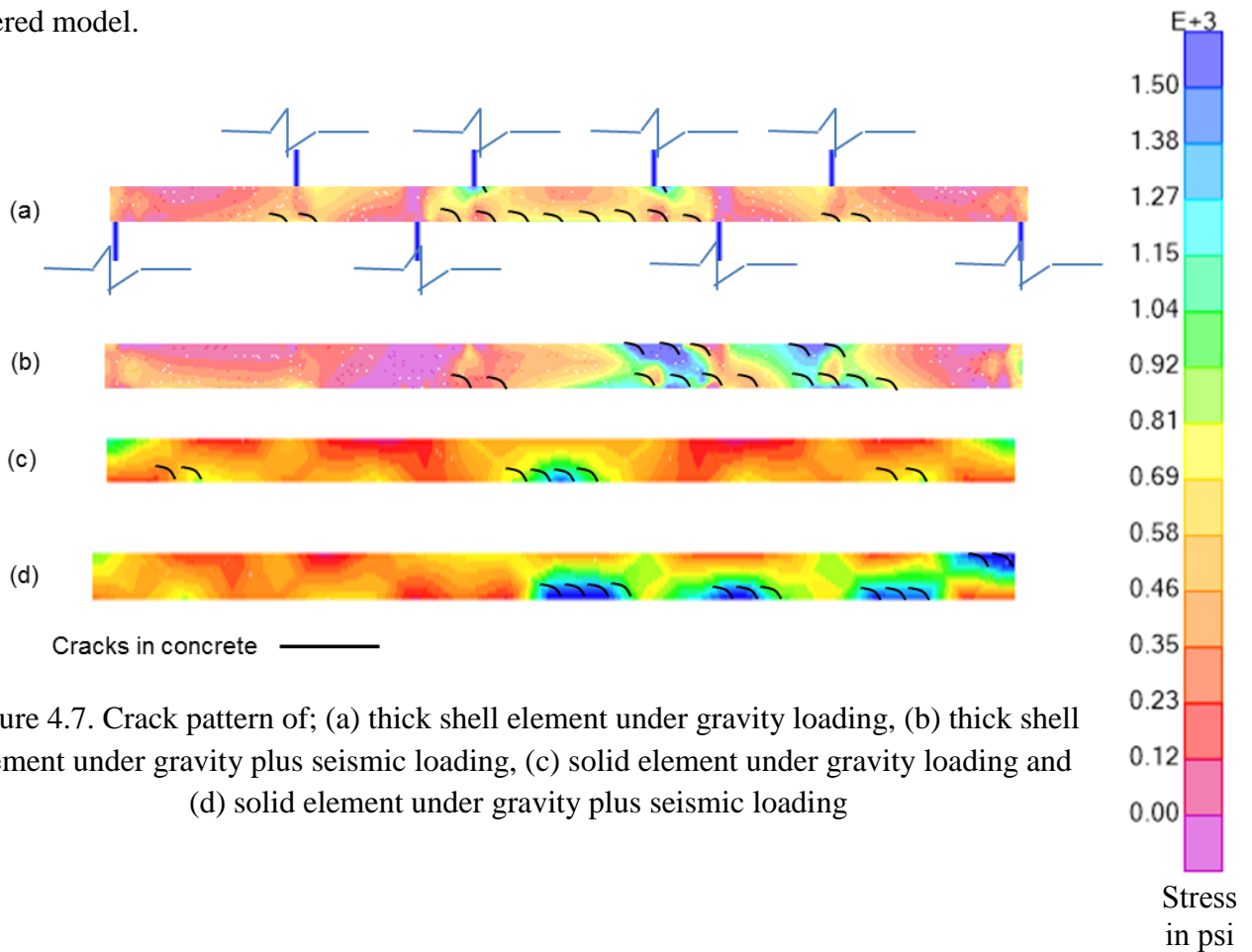
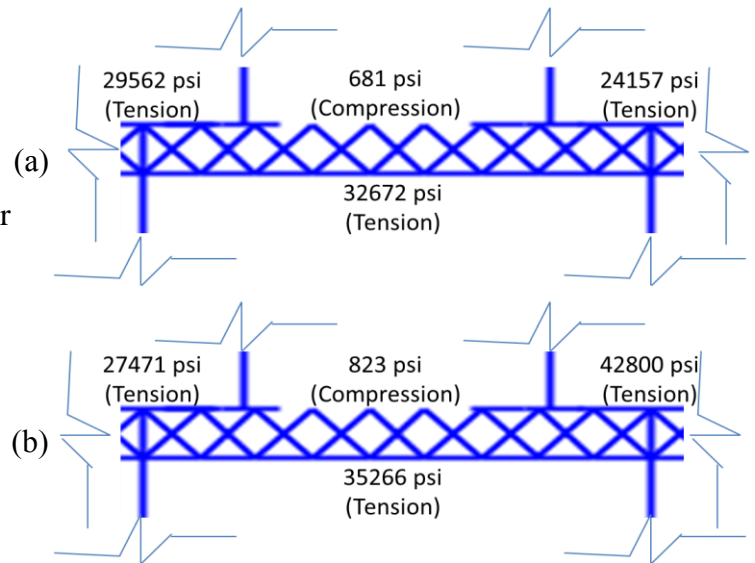


Figure 4.7. Crack pattern of; (a) thick shell element under gravity loading, (b) thick shell element under gravity plus seismic loading, (c) solid element under gravity loading and (d) solid element under gravity plus seismic loading

In case of thick shell/area model, the concrete stress exceeded its tensile strength by 27% at few locations under gravity loading. The maximum tensile stress is observed at top and bottom of TG below the core wall as shown in Figure 4.7(a). Under the gravity plus seismic loading, the concrete stress exceeded the tensile strength by 46% at many locations which mean that the cracks may be developed in TG, particularly below core wall as shown in Figure 4.7(b). In case of solid/3D model, the concrete is reached to its maximum tensile strength by 22% under gravity loading as shown in Figure 4.7(c). Under gravity plus seismic loading, the concrete stress exceeded the tensile strength at few locations by 42% as shown in Figure 4.7(d). It may be noted that the crack pattern of non-linear shell layered model, thick shell/area and solid/3D model is almost the same with respect to location. As the maximum stress is observed below core wall in different models discussed above therefore, STM is checked below core wall only. The compressive stress in concrete struts and tensile stress in steel ties under gravity and gravity plus seismic loading is shown in Figure 4.8(a) & (b), respectively. It may be noted that the ties at bottom of the TG reached to 54% under gravity loading and 58% under gravity plus seismic loading of its tensile strength. The struts reached to 18 % under gravity loading and 21% under gravity plus seismic loading of its compressive strength. The ties at the top of TG where columns of upper floors are supported, reached to 40-50% under gravity loading and 45-71% under gravity plus seismic loading of its tensile strength. As far as determination of cracking extent and their location is concerned, the solid element is the second most suitable modeling technique.

Figure 4.8. Maximum compressive stress in struts and tensile stress in ties of STM; (a) under gravity loading and (b) under gravity plus seismic loading



The values of maximum deflection at mid span of the TG below core wall for frame/line element, shell/area element, solid/3D element and STM are 0.2473 inches, 0.1869 inches, 0.2092 inches and 0.2163 inches, respectively. The deflections are almost the same for all cases.

The storey shears above TG obtained from the analysis of different modeling techniques are shown in Figure 4.9. The storey shears are compared to that of reference model (non-linear shell layered model). The storey shear for frame/ line element and solid/3D element are, respectively 8% and 13% less than that of non-linear shell layered element. The storey shears for shell/area element and STM are 1.3% and 1% more than that of non-linear shell layered element. Thus, STM is the second best model as far as storey shear is concerned.

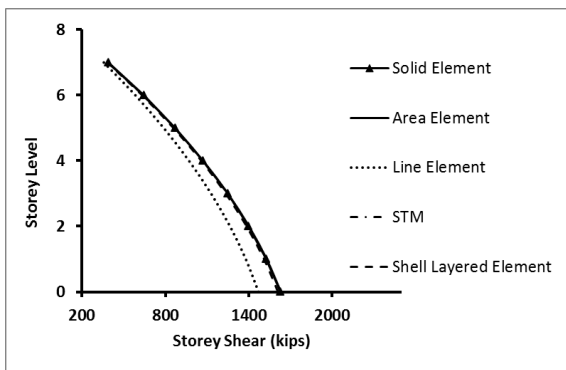


Figure 4.9. Storey shears of different modeling techniques for ESA

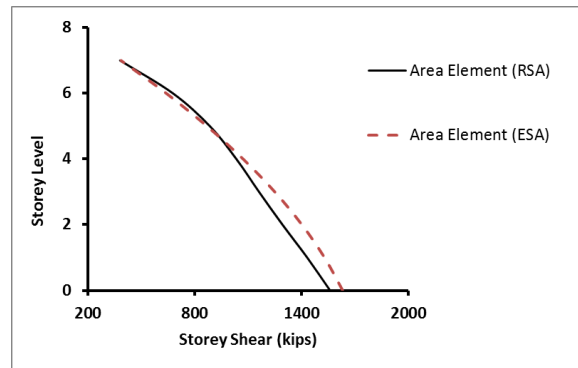


Figure 4.10. Storey shear of area element for RSA

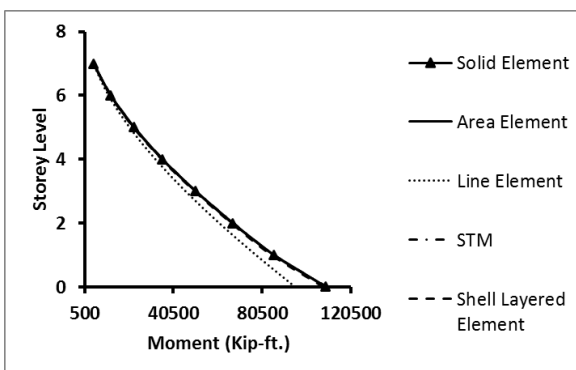


Figure 4.11. Overturning moments of different modeling techniques for ESA

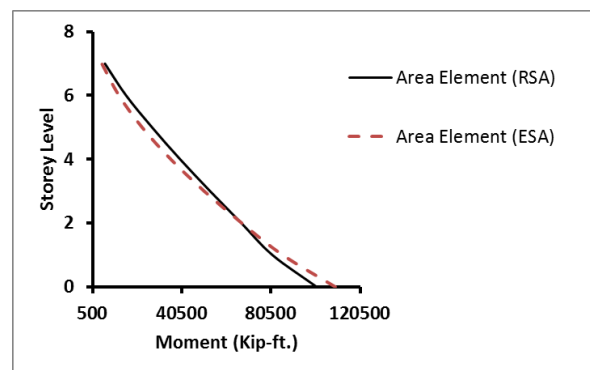


Figure 4.12. Overturning moments of area element for RSA

The overturning moments above transfer floor obtained from the ESA of different modeling techniques are shown in Figure 4.11.

The overturning moments are compared to that of reference model (non-linear shell layered model). The overturning moments for frame/ line element and solid/3D element are, respectively 11.8% and 11.5% are less than that of non-linear shell layered element. The overturning moments for shell/area element and STM, are respectively, 1.2% and 1.5% more than that of non-linear shell layered element. Thus, thick shell element is the second best model as far as overturning moment is concerned.

The storey drifts ratios obtained from the ESA using different modeling techniques are shown in Figure 4.13. The storey drift ratios of non-linear shell layered model is respectively 2.2% and 4.5% more than that of thick shell/area and solid/3D model and respectively 1.65% and 4.5% less than that of frame/line element and STM. Thus, thick shell element is the second best model as far as storey drift ratio is concerned.

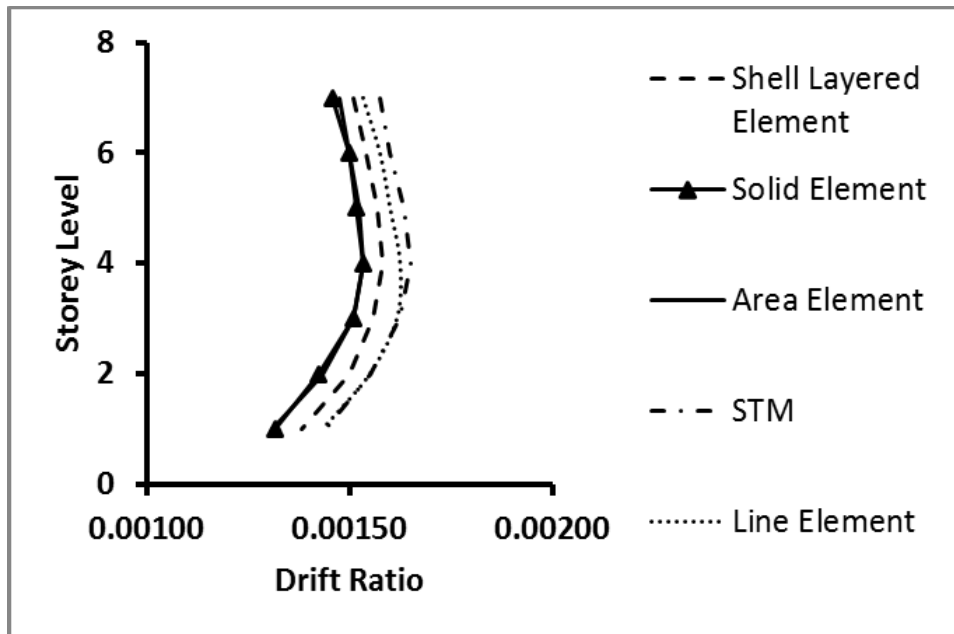


Figure 4.13. Storey drift ratios of different modeling techniques

Most of the parameters such as time period, storey drift, storey overturning moment, storey drift have 1-12% difference with reference model of non-linear thick shell element. Therefore, the stiffness modification factors suggested after small prototype beam study are seemed to be reasonable.

Tables 4.1 and 4.2 show the strain distribution at mid-span along the depth of the TG for different modeling technique under gravity and gravity plus seismic loading for ESA, respectively. The non-linearity of strain can be observed in the figures. The strain distribution from all modeling techniques resemble in respect of non-linearity with the experimental work of Niranjan and Patil (2012). The strain distribution along the depth of the line element under gravity loading would essentially linear considering the fact that its design is based on Whitney Stress block/linear strain distribution.

Tables 4.3, 4.5, 4.6 and 4.7 show the stress distribution along the depth of the TG for different modeling technique under gravity and gravity plus seismic loading for ESA. The stress distribution at mid span of the TG is plotted in Tables 4.3 and 4.6 under gravity and gravity plus seismic loading, respectively. Whereas, the stress distribution at the support is plotted in Tables 4.5 and 4.7 under gravity and gravity plus seismic loading for ESA, respectively. The non-linear distribution of stresses can be observed in the figures given in the above tables. The stress distribution for line element under gravity and for STM at supports was not drawn. The stress distribution from all modeling techniques resemble in respect of non-linearity with the experimental work of Holmes et al. (1972), Aftab (1965) and Niranjan and Patil (2012).

All the stress and strain diagrams are drawn as discussed in Chapter 03.

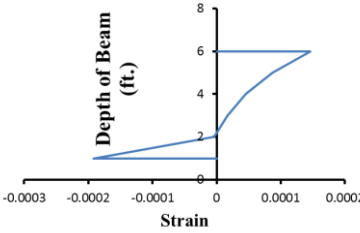
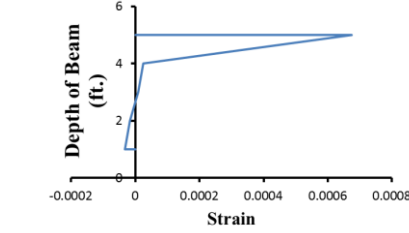
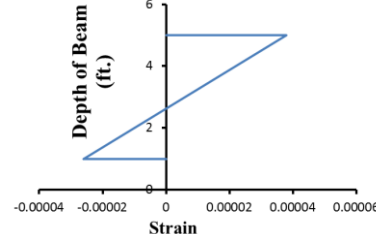
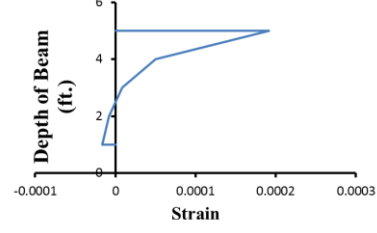
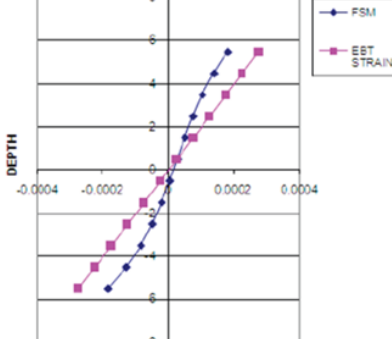
Model	Strain Distribution Diagram at Mid-Span
Frame/line	-----
Shell/area	
Solid/3D	
STM	
Non-linear shell layered	
Niranjan and Patel (2012)	

Table 4.1. Strain distribution diagrams at Mid-Span of different modeling techniques under gravity loading

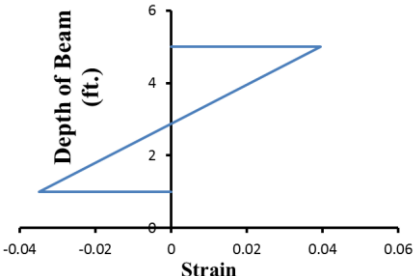
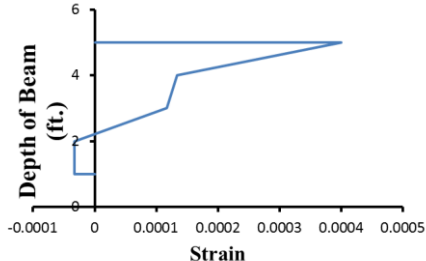
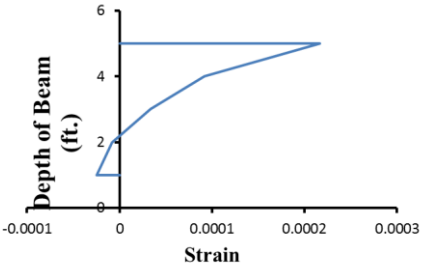
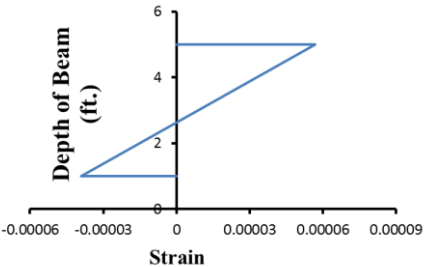
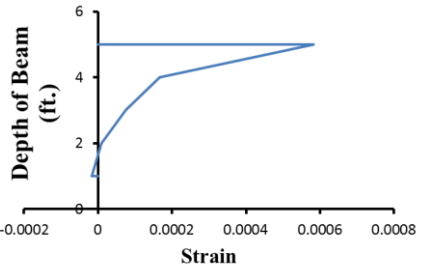
Model	Strain Distribution Diagram at Mid-Span
Frame/line	
Shell/area	
Solid/3D	
STM	
Non-linear shell layered	

Table 4.2. Strain distribution diagrams at Mid-Span of different modeling techniques under gravity plus seismic loading

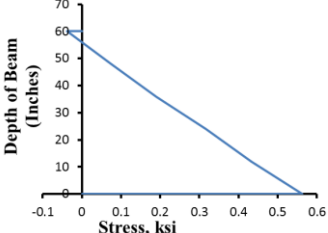
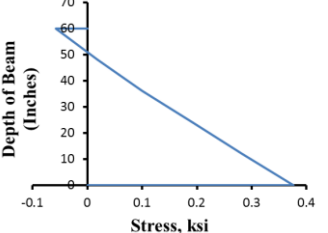
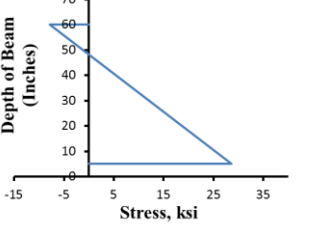
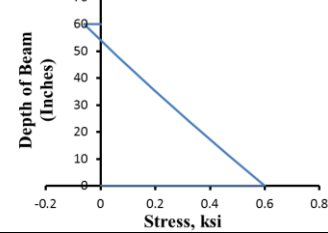
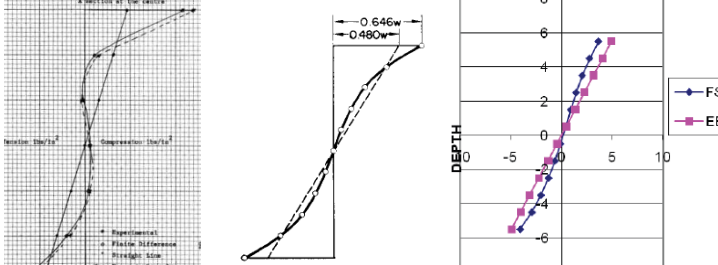
Model	Stress Distribution Diagram at Mid-Span
Frame/line	-----
Shell/area	
Solid/3D	
STM	
Non-linear shell layered	
Aftab (1965) Holmes (1972) Niranjan and Patel (2012)	

Table 4.3. Stress distribution diagrams at mid-span of different modeling techniques under gravity loading

Model	Stress Distribution Diagram at Support
Frame/line	-----
Shell/area	
Solid/3D	
STM	-----
Non-linear shell layered	

Table 4.4. Stress distribution diagrams at support of different modeling techniques under gravity loading

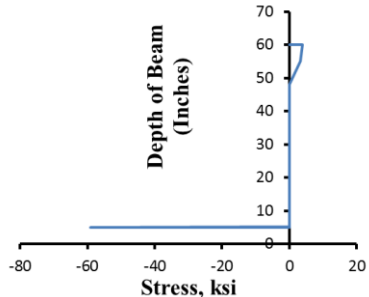
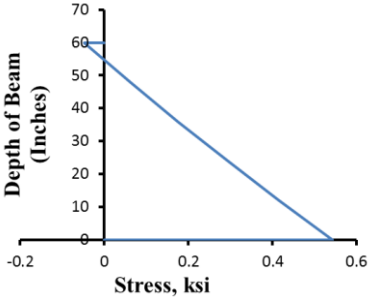
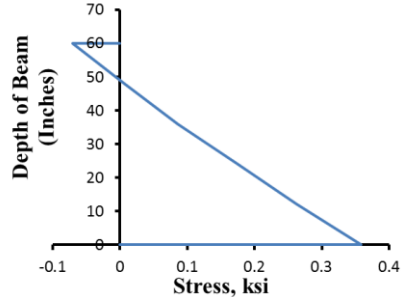
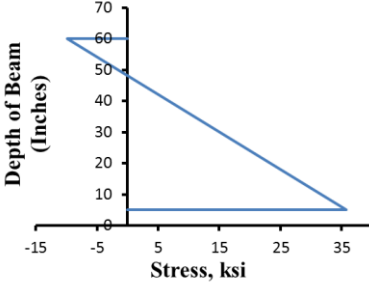
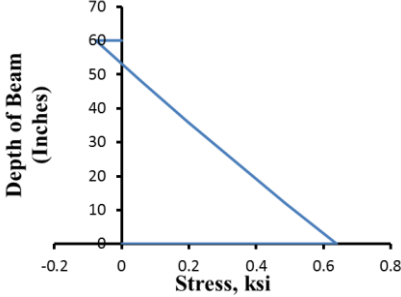
Model	Stress Distribution Diagram at Mid-Span
Frame/line	
Shell/area	
Solid/3D	
STM	
Non-linear shell layered	

Table 4.5. Stress distribution diagrams at mid-span of different modeling techniques under gravity plus seismic loading

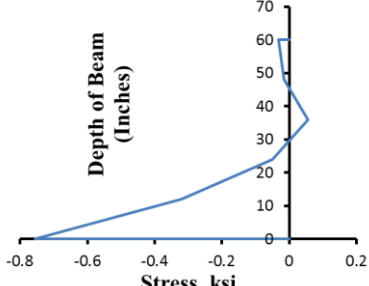
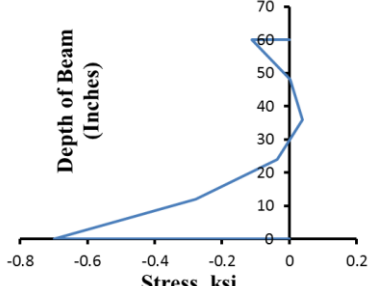
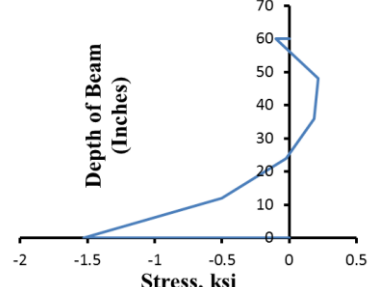
Model	Stress Distribution Diagram at Support
Frame/line	-----
Shell/area	
Solid/3D	
STM	-----
Non-linear shell layered	

Table 4.6. Stress distribution diagrams at support of different modeling techniques under gravity plus seismic loading

4.6 Summary of Case Study

The summary of the case study may be summarized as follows:

- The results of the prototype beam as discussed in previous chapter are extended to the 11-storied case study structure.
- The case study structure which contains 3 basements and ground+7 stories is located in seismic zone-04 and soil profile type-SD. Four (04) numbers of TGs are used in each direction. The grids pattern in basements is different from the grids pattern in the stories above.

- The TGs are modeled using different modeling techniques. The modification factors are used as worked out in case of prototype beam.
- All the reinforcement which is used later on in non-linear shell layered model is calculated by modeling the TG as a line element in SAP2000.
- Total numbers of 20 simulations are made for case study structure.
- The TGs are investigated against gravity loading and gravity plus seismic loading combinations.
- Various assessment methodologies such as ESA and RSA are used for computing seismic demands.
- The results obtained from ESA and RSA are comparable as the case study structure is regular structure and its height is less than less than 240 ft. Therefore, the results obtained from ESA are used for the further investigation.
- Time period, cracks pattern, maximum deflections, storey shears, overturning moments, storey drift ratios and, stress and strain distributions are compared for different modeling techniques.
- The bottom reinforcement stress reached up to 13% of its yielding strength under gravity loading and up to 33% under gravity plus seismic loading. The top reinforcement stress reached up to 9% of its yielding strength under gravity loading and up to 27% under gravity plus seismic loading. The shear reinforcement stress reached up to 5% of its yielding strength under gravity loading and up to 22% under gravity plus seismic loading.
- Among the available modeling techniques, non-linear shell layered modeling technique is recommended as the best modeling technique.

CHAPTER 5 SUMMARY, CONCLUSION AND RECOMMENDATIONS

5.1 Summary

For modern buildings, due to multi-functional requirements and architectural constraints, combined structural forms (which typically include shear wall systems in upper floors and moment-resisting frames together with basement retaining walls in lower floors), are commonly used. The lower floors of the buildings are typically used for parking, shopping malls, assembly halls, podium gardens or open spaces for functional requirements, while the upper floors generally accommodate apartments or shopping malls or offices. To accommodate this arrangement, the use of transfer structures between the lower floors and the upper floors of a high-rise building has become very popular. The span to depth ratio of transfer structures i.e. TG is normally less than 4; therefore, they fall under the definition of deep beams given by ACI-318-11. Existing methods of predicting deep beam behavior is based on either elastic theory or semi-empirical equation, none of which is entirely satisfactory (Yoo, et. al. 2004, Kong and Chemrouk, 2002). Typically a reinforced concrete beam is analyzed and designed by linear-elastic method. A stiffness modification factor is sometimes used to account the effect of cracking. However, the actual stresses distribution of a deep beam is non-linear (Hassoun and Al-Manaseer, 2008). The stiffness modification factor of 0.35 given in ACI code may not be correct for deep beams. Currently, ACI-318 does not provide equations for the design of non-linear stress distribution.

Therefore, suitable modeling techniques for transfer girders to assess the gravity and seismic behavior and suitable stiffness modification factors to account for the cracking effects, need to be investigated.

The main objectives of the study were to;

- Encourage the use of transfer structures i.e. TG in mix use buildings in high seismic zone.
- Present suitable modeling option of transfer girders i.e. line/frame element, area/shell element, solid/3D element, strut and tie model and non-linear shell layered element.
- Present stiffness modification factor for the assessment of the true gravity and combination of gravity plus seismic loading in mix use building structures.
- Discuss the seismic behavior of the transfer structure.

To ascertain the correct modeling technique compatible with failure mechanism and deflection of deep beam, the following methodology is adopted here:

- A small deep beam designed manually by strut and tie model, is verified analytically by different modeling techniques i.e. elastic line element, shell element, solid element, strut and tie modeling and non-linear shell layered element.
- Then, an 11 storied RCC structure with transfer girders at ground level, seismic zone-4 and soil profile type SD. Using the mentioned modeling techniques overall gravity and seismic behavior of the building is studied.
- Different parameters such as cracks pattern, maximum deflection, storey drift ratios, storey shears, overturning moments and stress & strain distribution are compared for each modeling technique.
- Various seismic assessment methodologies, including response spectrum analysis (RSA) and equivalent static analysis (ESA) are also use for seismic evaluation of the case study building.

5.2 Conclusion

The main conclusions of the study are underlined as under:

- The modulus of elasticity and shear modulus of concrete is recommended to be reduced to 20% to account for the effect of cracking on stiffness in case of frame/line element. For shell/area element, moment of inertia is recommended to be reduced to 35% of its gross value. For solid element, the modulus of elasticity and shear modulus of concrete is recommended to be reduced by 40%. In case of STM, a stiffness modification factor of 0.35 of moment of inertia for struts is recommended.
- In non-linear shell layered element model, the principal stress is almost 20% more than that of 460psi at the bottom of TG under gravity loading and 39% more than that of 460psi under gravity plus seismic loading. The bottom longitudinal reinforcement stress reached up to maximum 13% of the yielding strength, the top reinforcement stress up to 9% and the shear reinforcement stress up to 5% under gravity loading. Under gravity plus seismic loading the bottom, top and shear reinforcement stress reached to 33%, 27%, and 22% of yield strength respectively. The concrete in TG reached to 20% of its maximum crushing strain of 0.003.

- The tensile stress of concrete in shell/area and solid/3D model is 7% and 2%, respectively, more than that of non-linear shell layered model which is taken as a reference model under gravity loading and 3% and 7%, respectively, under gravity plus seismic loading.
- In case of STM, the ties at bottom of the TG reached up to 54% under gravity loading and 58% under gravity plus seismic loading of its yield strength. The struts reached up to 18 % under gravity loading and 21% under gravity plus seismic loading of concrete compressive strength. The ties at the top of TG where columns of upper floors are supported, reached up to 40-50% under gravity loading and 45-71% under gravity plus seismic loading of its yielding strength.
- Based on different parameters studied and previous experimental findings, the non-linear shell layered model is found to be the best technique to model the TG girder, whereas STM, thick shell, solid element and line element are better modeling options in preference starting from STM.
- The numerical modeling results show that reinforcement designed by the strut and tie method of ACI-318 is conservative confirming the findings of the previous researchers regarding the conservative design approach for deep beams of ACI-318. The reinforcement may be economized by using numerical model such as the non-layered shell element/STM model.
- This study is of practical nature which will help practicing engineers while designing these buildings/structures with deep beams on software's.

5.3 Limitations of the Study

The limitations of this study are;

- Only numerical modeling, analysis and design have been done.
- Only linear equivalent static analysis (ESA) and response spectrum analysis is performed. Static pushover analysis or non-linear time history analysis is not performed.

Different parameters are qualitatively compared with experimental work found in literature i.e. no experimental work is performed.

5.4 Recommendations for Future Work

Equivalent Static Analysis and Response Spectrum Analysis were implemented in this study. Static pushover analysis or non-linear time history analysis may be done to get clearer insight to the seismic behavior of super structure resting on transfer girders.

REFERENCES

- ACI (American Concrete Institute) 2008/ACI 318-11. Building Code Requirements for Reinforced Concrete, 2011, *American Concrete Institute, Farmington Hills, MI, USA*.
- ACI (American Concrete Institute) Task committee., (1973). *American Concrete Institute, Farmington Hills, MI, USA*.
- Aftab, A., (1965). Stresses in Deep Beams. *MS Thesis, Department of Civil Engineering, McGill University, Montreal, Canada*.
- Aguilar, G., Matamoros, A. B., Parra-Montesinos, G. J., Ramírez, J. A., & Wight, J. K. (2002). Experimental evaluation of design procedures for shear strength of deep reinforced concrete beams. *ACI Structural Journal*, 99(4), 539-548.
- Al-Shraify, B I., (2005). Nonlinear Finite Element Analysis of Continuous Deep Beam on Elastic Foundation. *M.Sc. Thesis, Faculty of Engineering, Nahrain University, Baghdad, Iraq*.
- Arabzadeh, A., Rahaie, A. R., & Aghayari, R. (2009). A simple strut-and-tie model for prediction of ultimate shear strength of rc deep beams. *International Journal of Civil Engineering*, 7(3), 141-153.
- Bakir, P. G., & Bodurođlu, H. M. (2005). Mechanical behaviour and non-linear analysis of short beams using softened truss and direct strut & tie models. *Engineering Structures*, 27(4), 639-651.
- Bathe, K. J., & Wilson, E. L. (1976). Numerical methods in finite element analysis.
- Birrcher, D., Tuchscherer, R., Huizinga, M., Bayrak, O., Wood, S. L., & Jirsa, J. O. (2009). *Strength and Serviceability Design of Reinforced Concrete Deep Beams* (No. FHWA/TX-09/0-5253-1).
- British Standards Institution. (2004). *Eurocode 2: Design of Concrete Structures: Part 1-1: General Rules and Rules for Buildings*. British Standards Institution.
- Chemrouk, M., & Kong, F. K. (2004). Diagonal cracking and ultimate shear strength of slender high strength concrete deep beams. *Advances in Structural Engineering*, 7(3), 217-228.
- CSI (Computer Structure International Analysis Reference Manual /CSI 2011)
- De Silva, C. W. (Ed.). (2005). *Vibration and shock handbook*. CRC Press.
- Dirar, S. M. O. H., & Morley, C. T. (2005). Nonlinear finite element analysis of reinforced concrete deep beams. In *Proceedings of VIII International Conference on Computational Plasticity, Complas VIII, Barcelona*.

- Enem, J. I., Ezech, J. C., Mbagiorgu, M. S. W., & Onwuka, D. O. (2012). Analysis of deep beam using Finite Element Method. *International Journal of Applied Science and Engineering Research*, 1(2), 348-356.
- FU, C. C., (2001). The Strut-and-Tie Model of Concrete Structures. *The Maryland State Highway Administration*.
- Geer, E. (1960, January). Stresses in deep beams. In *Journal Proceedings* (Vol. 56, No. 1, pp. 651-662).
- Hassoun, M. N., & Al-Manaseer, A. (2008). Shear and Diagonal Tension. In Reinforced Concrete, *Mechanics and Design 4th Edition*, New Jersey, John Wiley & Sons.
- Kuang, J. S., & Puvvala, J. (1996). Continuous transfer beams supporting in-plane loaded shear walls in tall buildings. *The Structural Design of Tall Buildings*, 5(4), 281-293.
- Li, J. H., Su, R. K. L., & Chandler, A. M. (2003). Assessment of low-rise building with transfer beam under seismic forces. *Engineering Structures*, 25(12), 1537-1549.
- MacGregor, J. G, Wight, J. K., (2005). Discontinuity Regions and Strut-and-Tie Models. *Reinforced Concrete Mechanics and Design Fourth Edition*, Upper Saddle River, New Jersey, Pearson Prentice Hall.
- Mander, J. B., Priestley, M. J. N., & Park, R. (1984). Seismic design of bridge piers. *Research Report, Department of Civil Engineering, University of Canterbury, Christchurch, New Zealand*.
- Masab, A., Saad, I., & Mubashar R., (2014). Comparison of Shear Behavior of Light Weight and Normal Weight Concrete Deep Beams. *MS Thesis, Department of Civil Engineering, University of Engineering and Technology, Taxila, Pakistan*.
- Matamoros, A. B., & Wong, K. H. (2003). Design of simply supported deep beams using strut-and-tie models. *ACI Structural Journal*, 100(6), 704-712.
- Niranjan, B. R., & Patil, S. S. (2012). Analysis of RC Deep Beam by Finite Element Method. *International Journal of Modern Engineering Research (IJMER)*, 2(6).
- NOJIRI, M. I. T. S. Y., & AKIYAMA, H. (1985). Experimental studies on shear strength of large reinforced concrete beams under uniformly distributed load. *Concrete Library International*, 5, 137.
- Park, R., & Paulay, T. (1975). *Reinforced concrete structures*. John Wiley & Sons.

- Quintero-Febres, C. G., Parra-Montesinos, G., & Wight, J. K. (2006). Strength of struts in deep concrete members designed using strut-and-tie method. *ACI Structural Journal*, 103(4), 577.
- Rahal, K. N., & Al-Shaleh, K. S. (2004). Minimum transverse reinforcement in 65 MPa concrete beams. *ACI Structural Journal*, 101(6), 872-878.
- Rao, G. A., Kunal, K., & Eligehausen, R. (2007). Shear strength of RC deep beams. In *Proceedings of the 6th International Conference on Fracture Mechanics of Concrete and Concrete Structures* (Vol. 2, pp. 693-699).
- Russo, G., Vanir, R., & Pauletta, M. (2005). Reinforced Concrete Deep Beams--Shear Strength Model and Design Formula. *ACI Structural Journal-American Concrete Institute*, 102(3), 429-437.
- Schlaich, J., Schafer, K., & Jennewein, M., (1987). Towards a Consistent Design of Structural Concrete. *PCI Journal*: 74-150.
- Sciammarella, C. A. (1963). *Effect of holes in deep beams with reinforced vertical edges*. Florida Engineering and Industrial Experiment Station, College of Engineering, University of Florida.
- Sheikh, M. A., dePaiva, H. A., & Neville, A. M., (1971). Flexure-Shear Strength of Reinforced Concrete Deep Beams. *The Structural Engineer*, 49: 359-363.
- Singh, B., Kaushik, S. K., Naveen, K. F., & Sharma, S. (2006). DESIGN OF A CONTINUOUS DEEP BEAM USING THE STRUT AND TIE METHOD. *ASIAN JOURNAL OF CIVIL ENGINEERING (BUILDING AND HOUSING)*, 7(5), 461-477.
- Su, R. K. L. (2008). Seismic behaviour of buildings with transfer structures in low-to-moderate seismicity regions. *Department of Civil Engineering, The University of Hong Kong, Hong Kong, China*.
- Su, R. K. L., & Cheng, M. H. (2009). Earthquake-induced shear concentration in shear walls above transfer structures. *The Structural Design of Tall and Special Buildings*, 18(6), 657-671.
- Tan, K. H., Tong, K., & Tang, C. Y. (2003). Consistent strut-and-tie modelling of deep beams with web openings. *Magazine of Concrete Research*, 55(1), 65-75.

- Tang, T. O., & Su, R. K. L. (2015). Gravity-induced shear force in reinforced concrete walls above transfer structures. *Proceedings of the Institution of Civil Engineers-Structures and Buildings*, 168(1), 40-55.
- Timoshenko, S. P. (1921). LXVI. On the correction for shear of the differential equation for transverse vibrations of prismatic bars. *The London, Edinburgh, and Dublin Philosophical Magazine and Journal of Science*, 41(245), 744-746.
- Trifunac, M. D., & Todorovska, M. I. (2008). Origin of the response spectrum method. In *Proceedings of the 14th world conference on earthquake engineering* (pp. 12-17).
- Van Thuat, D. (2013). Storey strength demands of irregular frame buildings under strong earthquakes. *The Structural Design of Tall and Special Buildings*, 22(9), 687-699.
- Wang, Q., & Hoogenboom, P. C. J. (2004). Nonlinear analysis of reinforced concrete continuous deep beams using stringer-panel model. *Asian Journal of Civil Engineering (Building and Housing)*, 5(1-2), 25-40.
- Wu, M., Qian, J., Fang, X., & Yan, W. (2007). Experimental and analytical studies on tall buildings with a high-level transfer storey. *The Structural Design of Tall and Special Buildings*, 16(3), 301-319.
- Yang, K. H., Chung, H. S., Lee, E. T., & Eun, H. C. (2003). Shear characteristics of high-strength concrete deep beams without shear reinforcements. *Engineering Structures*, 25(10), 1343-1352.
- Yoo, T. M., Doh, J. H., Guan, H., & Fragomeni, S. (2007). Experimental work on reinforced and prestressed concrete deep beams with various web openings.
- Zararis, P., (2003). Shear compression failure in reinforced concrete deep beams. *Journal of Structural Engineering* 129(4): 544-553.
- Zhua, Y., & Sub, R. K. L., (2008). Influence of Local Deformations of Transfer Structures on Seismic Design. *The 14th World Conference on Earthquake Engineering, Beijing, China.*

Comments:

Internal Examiner's Comments	Response
English grammar must be improved throughout the thesis.	Throughout thesis
Citation and reference list must be corrected.	
Reference style must be made consistent.	See references list
Summary of chapters 2, 3 and 4 should be included in their respective chapters.	See pages no. 22, 40 and 63
Tables should be included in thesis. Suggestions are given at appropriate locations. These all comparative tables. Comprehensive bar graphs are also helpful.	See pages no. 35, 37, 39, 57, 58, 59, 60, 61 and 62
Literature review should be done in a systematic way i.e. to discuss different aspects as are required later on chapter 3 and 4.	See chapter 02
How many total simulations are being made?	See pages no. 40 and 60
Annexures may be included showing the results not presented in thesis.	Significant results are presented in thesis
Abstract is too short. It should be at least one page long.	See abstract
List of symbols and notations should be included.	See page no. viii
Terminologies should be made consistent.	Checked throughout the thesis
Quality of few photos should be enhanced.	Has been enhanced see pages no. 10, 14 and 18
Results of all studied models (directly or indirectly) should be discussed in chapter 3.	See chapter 03
Additional certain plans should be included in case study structures. Suggestions are given on back of relevant pages in chapter 4.	See page no. 44
It is not clearly mentioned that results of whole analysis ESA or RSA are being presented in chapter 4.	See page no. 49
Results of all models for all parameters should be discussed. In case, results of few models for certain parameters are not discussed. It should be clearly mentioned in respective sections.	See pages no. 37, 39, 57, 58, 59, 60, 61 and 62
Expected reasoning for the observed behavior should also be mentioned in each studied parameters.	See chapter 04
No details are provided about the case study structure regarding structural member sizes, loading and loading combinations etc.	See page no. 45
Are all columns, shear walls and beams designed?	Yes
External Examiner's Comments	Response
Does the matching of only the cracks pattern is good enough? What about stresses, strains and deflections?	See pages no. 35 and 36
Any explanations for modifying stiffness modification factors?	See page no. 36
Clarification of seismic loading?	See page no. 44
What the examiners understand is:	
For chapter 3, there are five models of prototype beam analyzed under gravity loading. Taking mid-span deflection of non-linear shell layered element as reference, modification factors of other models are determined by hit and trial.	This is exactly what I did
For chapter 4, there are five models of case study structures analyzed under (i) gravity loading and (ii) combination of gravitational loading (it is not clear whether it is ESA or RSA). So results are for either 5x2 or 5x3 i.e. 5 being the number of models and 2 or 3 being are numbers of analysis being made.	It is 5x2 because RS case was only checked once for the comparison
All studied parameters should be discussed in Abstract, Introduction and Literature review chapters.	Has been discussed